



ESO/STC-601  
Date: 06.10.2017

## EUROPEAN ORGANISATION FOR ASTRONOMICAL RESEARCH IN THE SOUTHERN HEMISPHERE

---

La Silla Paranal Committee Meeting 23 October 2017	<b>For Information</b>
Scientific Technical Committee 90 <sup>th</sup> Meeting 24 and 25 October 2017	<b>For Information</b>

### **Science Cases for a Visible MCAO Instrument**

This document is for **PUBLIC DISTRIBUTION**

Scientific Technical Committee is invited to note this document.



European Organisation for Astronomical Research in the Southern Hemisphere

**Programme:** PIP

**Project/WP:** PIP New III Instrument

## **Science Cases for a VLT Visible MCAO Instrument**

**Document Number:** ESO-299554

**Document Version:** 1

**Document Type:** Science Report (SRP)

**Released On:** 2017-10-05

**Document Classification:** Public

**Prepared by:** Kuntschner, Harald

**Validated by:** Leibundgut, Bruno

**Approved by:** Pasquini, Luca

Name



## Authors

Name	Affiliation
Harald Kuntschner	ESO
Eline Tolstoy	University of Groningen, NL
Anita Zanella	ESO
Celine Peroux	Laboratoire d'Astrophysique de Marseille, ESO (guest)
Simona Vegetti	MPA, Germany
Andrea Bellini	STScI, USA
Olivier Hainaut	ESO
Monika Petr-Gotzens	ESO

## Change Record from previous Version

Affected Section(s)	Changes / Reason / Remarks
1.0	First release



## Contents

1. Introduction .....	5
1.1 Scope .....	5
1.2 Definitions, Acronyms and Abbreviations.....	5
2. Related Documents .....	5
2.1 Applicable Documents .....	5
2.2 Reference Documents .....	6
3. Science Cases .....	7
3.1 Resolved Stellar Populations .....	7
3.1.1 Introduction .....	8
3.1.2 A science case for a new optical instrument.....	10
3.1.3 Technical Requirements: .....	16
17	
3.1.4 Summary .....	23
3.2 Solar System Science and Outreach .....	25
3.2.1 Planets .....	25
3.2.2 Cometary activity .....	26
3.2.3 Deep photometric observations .....	27
3.2.4 Small satellites .....	28
3.2.5 Rings.....	28
3.2.6 Outreach .....	29
3.3 Giant star-forming clumps at high redshift: the new viewpoint offered by visible AO on VLT.....	32
3.3.1 Introduction .....	32
3.3.2 Why is a new instrument needed .....	41
3.3.3 Summary .....	41
3.4 The hunt for intermediate-mass black holes in globular clusters .....	44
3.5 Spatially Resolved Absorption Lines .....	46
3.5.1 Background.....	46
3.5.2 Spatially Resolved Absorption Lines:.....	48
3.5.3 Technical Requirements (Desirables):.....	50
3.5.4 Competitors: .....	50
3.5.5 Potential Targets:.....	51
3.5.6 Conclusions .....	52
3.6 Detecting low-mass dark matter haloes with gravitational lensing.....	53
3.6.1 Introduction .....	53
3.6.2 Pushing down the mass function with a new optical instrument.....	58
3.6.3 Technical Requirements .....	59



3.6.4 Summary .....	60
3.7 Star formation science with an optical AO instrument at the VLT .....	62
3.7.1 The formation of multiple stars.....	62
3.7.2 Star formation in the LMC .....	65
4. Summary of science requirements.....	67
4.1 Place of installation .....	67
4.2 Observing modes .....	67
4.3 Adaptive optics.....	67
4.4 Scientific filters and spectral resolution.....	68
4.5 Pixel scales and FoV sizes .....	68
4.6 Wave-front sensors .....	68
4.7 Optical distortions.....	68
4.8 Detector.....	69
4.9 Integration times and depth.....	69



# 1. Introduction

## 1.1 Scope

This document summarizes the Science Cases for the VAOI (Visible AO Instrument) instrument during its pre-Phase Design in 2017. It contains a detailed description of the Science Case and establishes the Science Requirements. This is the first collection of science cases for this instrument.

The VAOI Science Case was prepared by the VAOI Instrument Scientist, together with the members of the VAOI Project Science Team: Eline Tolstoy (Univ. of Groningen, Netherlands), Anita Zanella (ESO), Celine Peroux (Marseille, ESO guest), Simona Vegetti (MPA, Germany), Andrea Bellini (STScI, USA), Olivier Hainaut (ESO) and Monika Petr-Gotzens (ESO).

## 1.2 Definitions, Acronyms and Abbreviations

This document employs several abbreviations and acronyms to refer concisely to an item, after it has been introduced. The following list is aimed to help the reader in recalling the extended meaning of each short expression:

AOF	Adaptive Optics Facility
DM	Deformable Mirror
E-ELT	European Extremely Large Telescope
FoV	Field of View
IFU	Integral Field Unit
TBC	To Be Clarified
TBD	To Be Defined
VAOI	Visible AO Instrument
WFS	Wave Front Sensor

# 2. Related Documents

## 2.1 Applicable Documents

The following documents, of the exact version shown, form part of this document to the extent specified herein. In the event of conflict between the documents referenced herein and the content of this document, *the content of this document shall be considered as superseding*.

AD references shall be specific about which part of the target document is the subject of the reference.

AD1 Requirements for Scientific Instruments on the VLT; [VLT-SPE-ESO-10000-2723](#), Version 1

AD2 Data Flow for VLT instruments Deliverables Specifications; [VLT-SPE-ESO-19000-1618](#) Version 3



## 2.2 Reference Documents

The following documents, of the exact version shown herein, are listed as background references only. They are not to be construed as a binding complement to the present document.

Not applicable



## 3. Science Cases

### 3.1 Resolved Stellar Populations

By *Eline Tolstoy, Kapteyn Astronomical Institute, University of Groningen, NL*

#### Abstract:

A Colour-Magnitude diagram (CMD) has long been a key astrophysical tool to accurately determine the star forming history of nearby galaxies. Improving sensitivity and resolution have over the years extended the distance and accuracy with which this approach can be applied. For most stars the spectral energy distribution peaks around the V-band optical region. This makes resolved stellar populations a clear-cut science case for imaging with improved spatial resolution and flux sensitivity at optical wavelengths. This encompasses numerous scientific questions of importance, and the benefit of opening a new parameter space in high resolution optical imaging that will bring additional exciting and unexpected results.

The potential for a diffraction-limited optical camera with a 30arcsec field of view and extensive sky coverage on the VLT would be dramatic if excellent image quality can be achieved and maintained, and the sensitivity increases with the spatial resolution. This would enable accurate CMDs of nearby galaxies going well beyond what the 2.4m HST, or 6.5m JWST, can achieve. The resolution would compare well with the infrared imaging capabilities of the E-ELT, as the diffraction limit of an 8m telescope in V-band matches that of a 40m telescope in K-band. A key science goal of MICADO/MAORY on the E-ELT is to extend accurate CMDs analysis to “normal” elliptical galaxies in the Virgo cluster (at ~17 Mpc) or Fornax cluster (at ~19Mpc). This goal is challenging with only infra-red wavelengths, as neither the colour baseline nor the flux sensitivity is optimum for most stellar populations. The surface brightness of the sky background reduces dramatically at optical wavelengths, compared to the infrared. This means that a diffraction limited optical camera on the VLT could be an excellent match to a diffraction limited infrared camera on the E-ELT, and the combination will benefit the study of resolved stellar populations at distances out to the Virgo or Fornax clusters.

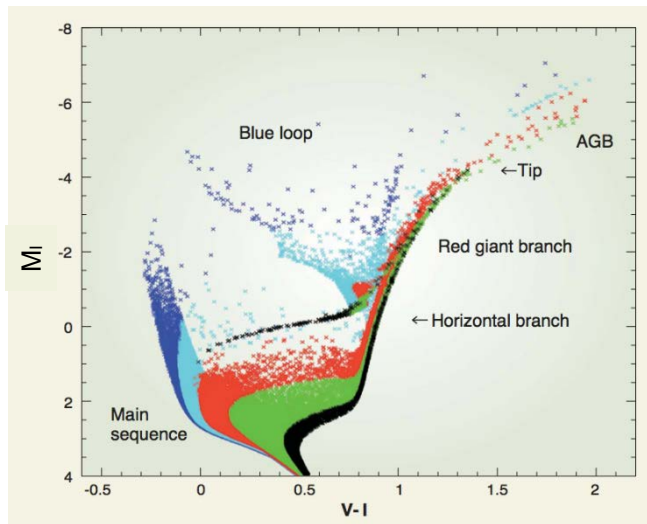


**Figure 1:** A simulation (with no errors) from stellar evolution models, of the CMD, of a galaxy that has constantly formed stars over the last 13 Gyr. The stars are colour-coded according to age: blue, stars <300 Myr old; cyan, 0.3 to 1.1 Gyr; red, 1.1 to 3 Gyr; green, 3 to 8 Gyr; black, >8 Gyr. Key stellar evolution phases that clearly mark the presence of stellar populations of different ages are labelled. Taken from Tolstoy (2011).

### 3.1.1 Introduction

The interpretation of an observed CMD allows us to determine stellar ages, masses and metallicities from the colours and magnitudes of individual stars in a stellar system. This is the most powerful tool to understand the global stellar properties and how they have varied over time in star clusters, the Milky Way and galaxies in and beyond the Local Group. Historically the study of resolved stellar populations in nearby galaxies enabled Edwin Hubble and others in the 1920s to realise that galaxies were at distances well beyond the boundary of the Milky Way (e.g., Hubble 1925). By the 1940s Walter Baade started to use the colours of resolved stars to distinguish between old and young stellar populations in Local Group galaxies (Baade 1944a,b). This field continues to transform and improve our understanding of stellar and galaxy evolution as telescope size and performance improves. The latest leap occurred with the advent of HST in the 1990s. The exquisite spatial resolution and sensitivity enabled the most detailed and precise CMDs of stellar systems extending beyond the Local Group (e.g., Tolstoy, Hill & Tosi 2009, and references therein; Weisz et al. 2014).

Past studies have clearly demonstrated the requirement for accurate and deep photometry (e.g. Cignoni & Tosi 2010). To obtain the full details of the star formation history of a galaxy going back to the earliest times, the oldest main sequence turnoff region ( $M_I \sim 3$ ; in Vega magnitudes) is required, as can be seen in Figure 1. The brighter red giant branch is clearly a poor age discriminator, whereas on the main sequence the different age groups are clearly distinct. The horizontal branch contains stars  $>10$  Gyr old and it is thus an unequivocal indicator of the presence of an ancient stellar population, but so far it has proved difficult to interpret in terms of a star formation history (Salaris et al. 2013), especially when it is sparsely populated, or over whelmed by younger populations (see Figure 2).

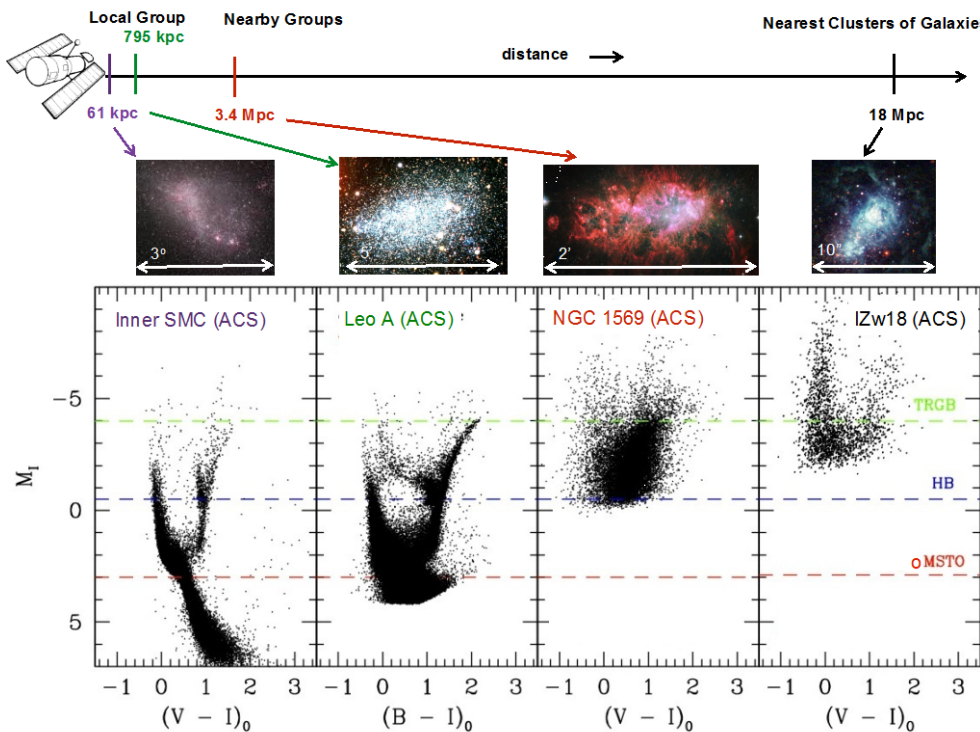


**Figure 2:** The deepest possible CMDs in absolute magnitudes of four different star-forming galaxies at increasing distances, based on 10s of orbits (except for the SMC) with the ACS on HST. The dashed lines show the position of the oldest Main Sequence Turnoff (oMSTO), the Horizontal Branch (HB) and the Tip of the Red Giant Branch (TRGB). The CMDs come from Cignoni et al. 2012 (SMC); Cole et al. 2007 (Leo A); Grocholski et al. 2012 (NGC 1569) and Aloisi et al. 2007 (I Zw 18). To convert the absolute magnitudes plotted for the CMDs in Figure 2 to observed apparent Vega magnitudes the value of the distance modulus needs to be added to  $M_I$ . This means +18.9 for the SMC; +24.5 for Leo A; +27.7 for NGC1569 and +31.3 for IZw18.

The limits of what is currently possible, with HST at increasing distances, is shown in Figure 2. As the distance increases the spatial scale compresses (as can be seen in the images of the galaxies at the top of Figure 2). In addition the sensitivity decreases with distance, as can be seen from the increasingly shallow observed CMDs in Figure 2 for further away galaxies. The CMDs for the more distant systems of course also have increasing photometric errors (more scatter) because of combined crowding and sensitivity limits. There are better CMDs for more distant galaxies, like Cen A, at 3.8Mpc (Rejkuba et al. 2011), but only for sparse fields in the halo of this galaxy.

The improvement in Adaptive Optics technology and the range of scientific applications to which it has been applied has also been impressive over the last years (e.g. Davies & Kasper 2012). Indeed the general case for optical AO has been made at an ESO conference (Davies et al. 2015), and the technical case has been further developed at SPIE (e.g. Esposito et al. 2016). There are a number of very compelling science cases to be made.

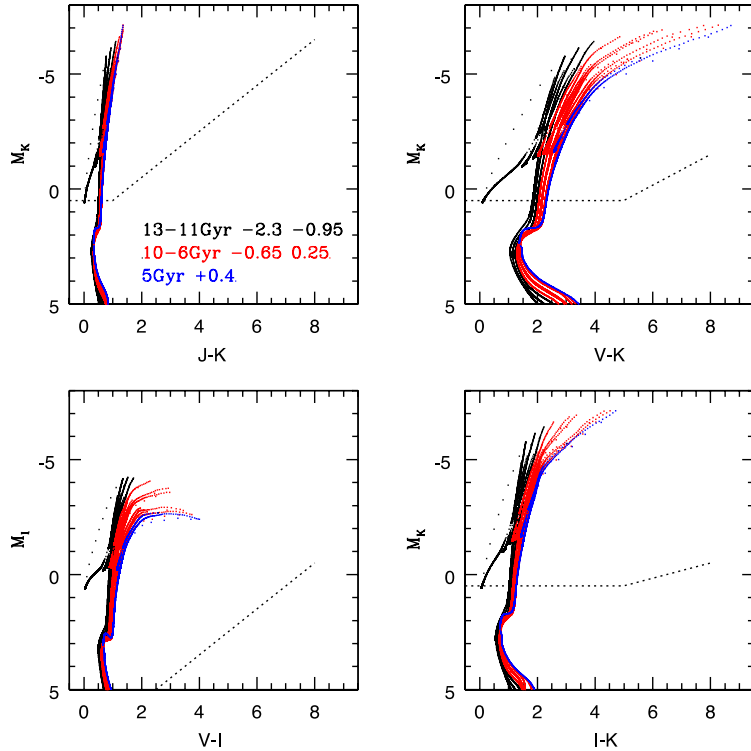


**Figure 3:** Teramo theoretical isochrones (Pietrinferni et al. 2004) in absolute Vega magnitudes for stars with a range of ages and metallicities (given in the upper left hand plot). All plots are for the same stellar population, but different filter combinations. The dotted straight lines are roughly the photometric limit that could be achieved in 10hrs, at S/N~5 and a distance of 1.7 Mpc with an HST where the K sensitivity would match H.

### 3.1.2 A science case for a new optical instrument

The major science driver for an instrument that can work at the V-band diffraction limit of a VLT is deep and accurate CMDs of resolved stellar populations, down to the oldest main sequence turnoffs, beyond the Local Group (as shown in Figures 1 & 2). This will allow us to tackle several fundamental questions for different galaxy types in different environments (e.g., in the Sculptor and Centaurus groups; the Virgo and Fornax clusters; fields galaxies). Most galaxies in the Local Group have been observed with HST, although some of the more dense central regions of larger galaxies (e.g., WLM, NGC3109, in the southern hemisphere) and various individual globular clusters have very noisy or not very deep CMDs and so require higher spatial resolution observations. Beyond the Local Group the first region of major interest to be explored in the southern hemisphere is the Sculptor group of galaxies, at a range of distances from 2-4 Mpc., thus with distance moduli in the range  $(m-M)_V \sim 26.5-28$ . This requires sensitivities going down to  $V \sim 29.5$  in Vega magnitudes for a diffraction limited VLT imaging of the main sequence turnoff region in the optical (see Figure 3). This will allow detailed studies of the resolved stars in bars, bulges, spiral arms, starbursts, globular and other star clusters in the Sculptor group to compare to the more limited sample

currently available in the Local Group. Less accurate CMDs will be available for yet more distant galaxies.

In this section we develop 4 different science cases, explaining the requirements for a diffraction limited optical imager at the VLT. There are of course many more possible applications, but those chosen here are considered to be those most likely to lead to major breakthroughs in our understanding of galaxy formation and evolution.

### 3.1.2.1 Is the Milky Way a typical Spiral galaxy?

If it is possible to resolve and detect individual stars in galaxies beyond the Local Group, then it is possible to determine accurate star formation histories of a range of different types of galaxy in different environments. A critical question that this will allow us to answer is: how representative are the Milky Way and M31 of galaxy formation and evolution processes everywhere in the Universe? This is a key aspect of our understanding of galaxy formation and evolution. This means looking at the properties of star formation in the disk galaxies, star by star, as deep CMDs allow a very accurate comparison to be made between older and younger stellar populations. It can also allow an accurate estimate of the metallicities of these different populations. In the Milky Way we have extraordinarily detailed information about the stellar populations, and once Gaia finishes its mission successfully we will have the correct context for all our measurements of individual stellar properties, as the distances of stars are very difficult to determine with great certainty beyond the solar neighbourhood. This will come in the next 5-7 years, and revolutionise our understanding of the Milky Way, however we will still need to know if the Milky Way is a typical spiral galaxy, or peculiar in some way. This requires comparison studies with external spiral galaxies, most of which are beyond the Local Group. M31 is the closest comparison, and with deep HST imaging of small areas in the outer disk it is possible to determine detailed star formation histories and age-metallicity relations (Bernard et al. 2015), see Figure 4, which suggest significant differences with the properties of the Milky Way outer disk (note that M31 is not accessible from the VLT). The Sculptor group will be a key testing ground, as it contains a number of spiral galaxies (e.g. NGC300, NGC247, NGC7793, NGC55), including a starburst spiral galaxy (NGC253). It should also be possible to go beyond the Sculptor group and make a statistically meaningful sample of galaxies that can be studied in this detail.

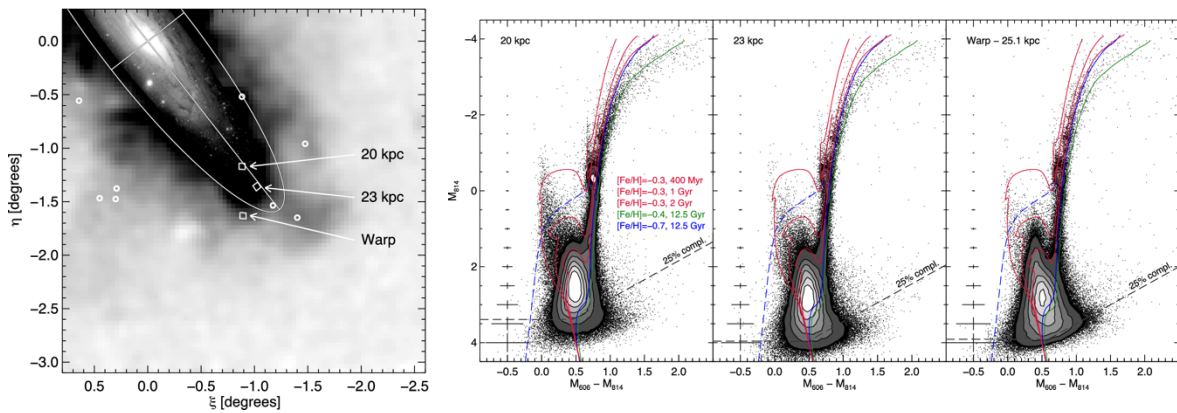


**Figure 4:** The location of HST/ACS pointings, with around 4 hours of total integration in each filter, superimposed on an INT/WFC map of the inner halo of M31. The CMDs for the three fields marked as open squares, are shown on the right. The open circles represent some of the fields that have been previously studied with HST. From Bernard et al. (2015).

The Sculptor group also contains a large range of smaller dwarf type galaxies, some of which are very compact, and for which the detailed star formation histories from CMDs down to the oldest main sequence turnoffs can be compared to similar studies in the Local Group. In this way the star forming properties of the satellites and the larger host can be compared in a different environment. This is another area where we need to understand how typical is the Milky Way and M31 and their satellites, which has important implications for our models of the effect of satellite merging and accumulation (e.g. Belokurov & Koposov 2016). These kinds of study all require higher spatial resolution than is possible with HST or JWST with high flux sensitivity to ensure CMDs of galaxies beyond the Local Group match those for galaxies in the Local Group (see Figure 2). It is well known that dwarf galaxies in the Local Group have a wide variety of different properties even at the same mass (e.g., Simon & Geha 2007; Tolstoy, Hill & Tosi 2009; Weisz et al. 2014). We don't know if this is universally true and if there is a relation with the host mass or other environmental factors.

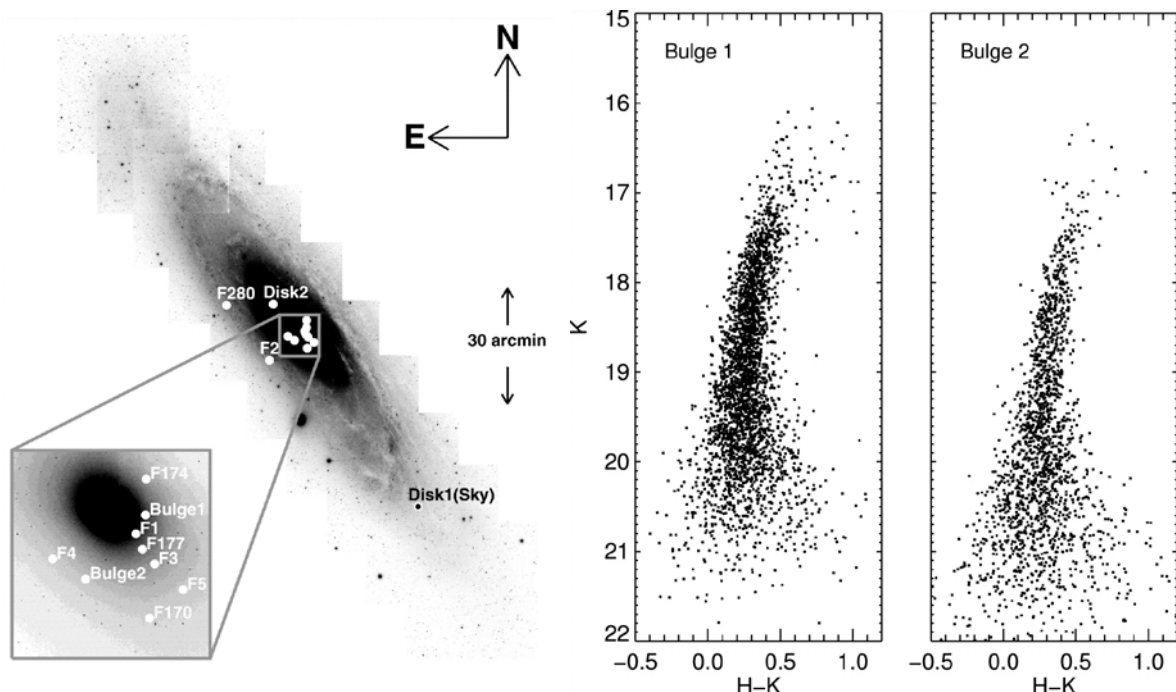


**Figure 5:** A study of the bulge of M31 with ALTAIR/NIRI on Gemini-North. On the left, are the locations of the fields imaged in the disk and bulge. On the right are the CMDs for the two bulge fields. These images have integration times of 400sec and spatial resolutions of 0.10arcsec (H), and 0.09arcsec (K) at radii within 9arcsec of the central guide star. From Olsen et al. (2006).

### 3.1.2.2 How do bulges vary with galaxy type?

It is also important to be able to resolve the individual stars in the bulges of a range of different galaxy types, with differing bulge-to-disk ratios, to determine the detailed age-metallicity distribution and potentially also the kinematics of the individual stars in these different systems. This will make it possible to distinguish between different formation mechanisms. The bulge is an important stellar component of most large galaxies and there are competing theories to explain the origin. They could be truly ancient stellar populations formed by early merging, or dynamical friction of the star forming clumps in the primordial disk or other disk instabilities. These different origins will result in different properties of the resolved stellar populations. For example to understand the role of the disk the bulge



properties need to be compared to the detailed resolved stellar properties of the disk. In the Milky Way individual stars can be resolved in the bulge, but there is considerable difficulty to gain a perspective and to be sure we have a clean bulge sample, as we need to look through the Galactic disk, and a lot of contamination from disk stars and dust extinction. Distinguishing between disk and bulge stars is easier in an external galaxy, especially where the orientation allows the clear separation between disk and bulge. Thus current theories of the relation between the disk and the bulge may be caused by confusion in the Milky Way, and in the end the Milky Way is only one galaxy. It is clear from the range of size and luminosity of the bulges in different galaxies, even of the same total luminosity, that detailed stellar properties must vary. The main difficulty in resolving the bulges of external galaxies is the high surface brightness, and thus severe crowding. This can be seen even in the case of HST and Gemini Infrared AO observations of M31 (Davidge et al. 2005; Olsen et al. 2006), see Figure 5. The marked differences between the CMDs in Figures 4 and 5 are due to the challenges of working in the infrared (see Figure 3), and are also an indication of the exponentially increasing crowding as we move further in towards the centre of M31. In addition, the ground-based infrared images of M31 have integration times of 400sec per filter, which is only ~2% of the HST optical images in Figure 4 (which are in excess of 4 hours per filter). Crowding prevents deeper integrations in this case, and this can only change with much better spatial resolution than HST or JWST can offer. Diffraction limited optical imaging with an 8m-class should go much deeper than is possible in the infrared or with HST. It also shows the importance of being able to build up sensitivity with longer integrations or stacked images. This is currently difficult with infrared AO imaging as the PSF varies too strongly with time.

### 3.1.2.3 What is the detailed star formation history of a “normal” elliptical galaxy?

All known “normal” elliptical galaxies are too distant and/or too crowded for a detailed CMD analysis. One of the major unknowns in our understanding of galaxy formation and evolution is the detailed evolutionary history of this type of galaxy. It is clear that integrated light studies, whilst highlighting their global properties, miss the all important fine details that only resolved stellar populations, in the form of CMD analysis, can provide. There are a few nearby peculiar elliptical galaxies for which resolved stellar studies have been attempted with HST. For example, M32, NGC147, NGC185 dwarf ellipticals, at around 750kpc and Cen A, an unusual elliptical galaxy, that is actually classified as an SO, at 3.8Mpc. In the case of M32 the crowding is extreme, even staying away from the central regions (Monachesi et al. 2011) and in Cen A only the halo is sparse enough (Rejkuba et al. 2011), and even here the distance and to some degree the crowding, makes CMD analysis challenging. For NGC185 and NGC147 (Geha et al. 2015) the deep HST imaging only looks at a small fraction of the outer regions. The halo of any galaxy contains a very small fraction of the total stellar mass, and therefore does not necessarily represent the full evolutionary history of the galaxy, as it does not in the Milky Way. Thus we have never managed to look into the heart of an elliptical galaxy and accurately disentangle the different age and metallicity stellar populations that may be found there.

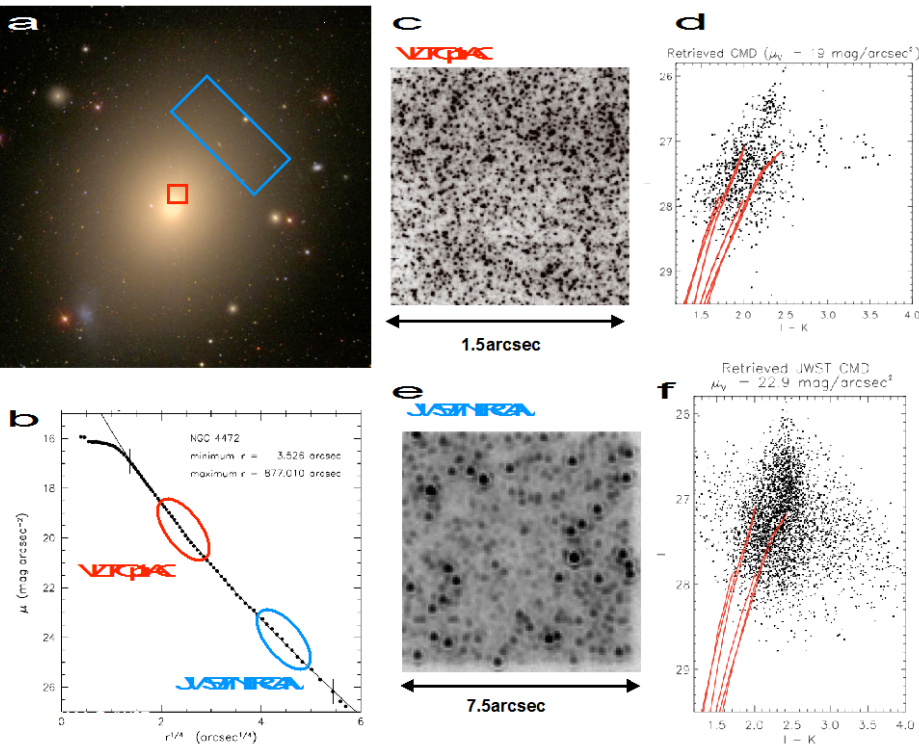


**Figure 6:** Here are shown (a) the regions of the Virgo elliptical galaxy NGC4472 (M79), a “typical” giant elliptical in the Virgo cluster that can be probed by a diffraction limited optical imager on the VLT or by MICADO in the infrared (red square, assuming a field of view of 50arcsec) and the area that can be probed by JWST (blue rectangle). These areas are positioned to reflect the surface brightness limit that can be resolved depending on the spatial resolution of the VLT (in V) and JWST in K; (b) the surface brightness profile of NGC 4472 (from Kormendy et al. 2009), showing the surface brightness accessible to VLT in V or MICADO in K (red ellipse) and JWST in K (blue ellipse), coming from simulations by Deep et al. (2011); (c) a simulated image of a small part of the field at the diffraction limit of an 8m telescope in the V-band for a position at,  $\mu_V \sim 19$  mag/arcsec $^2$ ; (d) the CMD coming from photometry of this image (in I, K filters, assuming that K comes from MICADO); (e) a simulated image in K of a small part of the field from JWST/NIRCAM at  $\mu_V \sim 23$  mag/arcsec $^2$ ; (f) the CMD coming from photometry of this image (in I, K filters). This figure is only a rough estimate, future versions will be updated.

The closest “normal” elliptical galaxies are in the Virgo cluster (at  $\sim 17$  Mpc distance). It is unlikely that the optical CMDs possible with the VLT at the distance of Virgo will reach the deepest main sequence turnoffs, and thus the synergy with the matching resolution and sensitivity in the infrared of E-ELT/MICADO will be critical for the interpretation of the resulting CMDs, by extending the colour baseline over the optical-infrared wavelength range (see Figure 3) to compensate for the lack of main sequence turn-off photometry. JWST will also be able to make (infrared) CMDs of Virgo elliptical galaxies, and with a larger field of view than MICADO or an optical AO instrument on the VLT, but because of its relatively limited spatial resolution, and collecting area, only at significantly larger distances from the central regions (see Figure 6), with a relatively bright magnitude limit, and thus for a small fraction of the total stellar population. These will also be infrared (K, J-K) CMDs, with the accompanying problems (see Figure 3). Figure 6 illustrates the situation. Recent

developments in interpreting Horizontal Branch stars in terms of the ancient star formation history look promising in this respect (Salaris et al. 2013), in that it might not be necessary to reach the oldest main sequence turnoffs, just the Horizontal Branch at  $M_V \sim -0.5$  (or  $V=30.5$  at Virgo or  $V=30.9$  at Fornax). The Fornax cluster is much smaller and slightly more distant than Virgo, but it also contains a range of elliptical, Spiral and S0 galaxies.

To be useful these observations would be extremely challenging for the VLT. They would require long exposures over many hours in very stable conditions. The (Vega-magnitude)  $V$ ,  $I$  sensitivities (in long exposures) would ideally reach  $V \geq 31$ mag to get the Horizontal Branch or below. If this (extraordinary) sensitivity cannot be achieved then  $V \sim 29.5$  will still allow the detection of the top 2.5mags of the red giant branch in a Virgo elliptical galaxy.

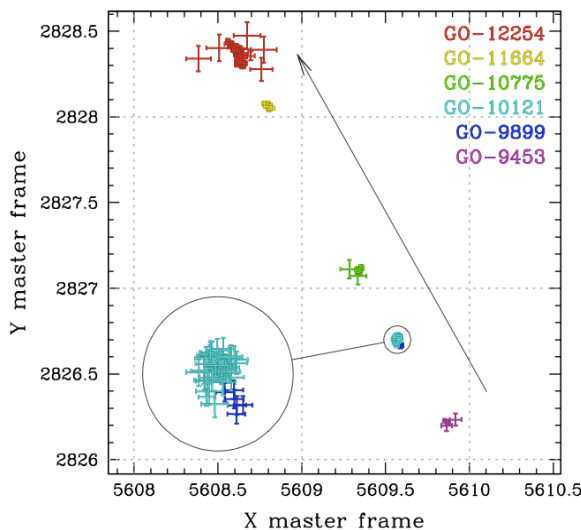


**Figure 7:** The individual star in the globular cluster NGC6752, measured over 6 HST epochs as they appear in the reference frame. Master-frame pixels are highlighted with dashed lines, so the axes are the pixel scale of the image. Star positions and error bars are colour coded according to the programme ID, which covers the period from 2002 to 2011. The black arrow shows the motion of the star in the plane of the sky over the 9 years of monitoring. The sizes of the error bars are related to the S/N of the measurements (some are short integrations). From Bellini et al. (2014).

### 3.1.2.4 Astrometry: dynamical masses and black holes

One interesting possibility, that is a high priority for MICADO, is astrometry. Being able to accurately measure how the positions of individual stars move with time has powerful potential in determining proper motions of entire stellar systems (e.g., globular clusters, dwarf galaxies), see Figure 7. In addition the relative motions of the stars within some systems can also be measured. This enables detailed dynamical information to be



extracted, such as the proper motion of the whole system in the plane of the sky, to determine the gravitational forces that are working on the stellar system as a whole. The internal proper motions of stars within a stellar system can be used to more accurately determine the mass of the entire system, and also to look for black holes in the high-density centres of stellar systems. Black holes lead to rapid motions of stars in their vicinity, as is seen in the Galactic centre (e.g., Genzel, Eisenhauer & Gillessen 2010). A diffraction limited optical imager on the VLT would allow this case to be extended well beyond the inner regions of the Milky Way. Of course working at the diffraction limit in optical wavelengths is only a benefit in systems that, unlike the Galactic centre, are not heavily extinguished by dust, which requires observations at infrared wavelengths. The more accurate and consistently positions of individual stars can be measured the more quickly and to greater distances proper motions can be measured.

### 3.1.3 Technical Requirements:

The prime example of a facility that made a huge impact in the field of resolved stellar populations is the (2.4m diameter) HST. This is because of the matched increase in flux sensitivity and spatial resolution compared to what was previously possible from the ground at optical wavelengths. HST also has the very important advantage over ground-based telescopes in that it operates in a stable environment, where the PSF barely changes over months and years. This makes it straightforward to increase flux sensitivity with long exposures. Matching space-based stability is challenging for a ground-based telescope, as the atmospheric conditions are constantly changing. It is possible that long exposures with a ground-based AO system will always require some kind of PSF reconstruction to accurately trace the variations in the PSF with time.

Currently the main limitation for ground based telescopes, like an 8.2m VLT UT, is that optical imaging is not possible near the diffraction limit (see Figure 8), over more than a few arcsec field of view, and this has very stringent requirements for on-axis (bright) guide stars within the field of view for tip-tilt corrections (e.g., SPHERE/ZIMPOL, Science Verification, R. Siebenmorgen/ESO). This guide star requirement severely limits the sky coverage available, and the tiny field of view makes it difficult to detect more than a handful of stars and then only in very particular positions on the sky. Diffraction limited wide-field ( $>20\text{arcsec}^2$ ) images on the VLT have been achieved with AO cameras at near-infrared wavelengths (e.g. MAD), however the observations still have quite demanding requirements for bright natural guide stars within the field of view. This guide star requirement has so far restricted the sky coverage to a very few special cases of resolved stellar population observations, which happen to have very bright stars in the field. Among even these restricted samples there have been interesting high-profile results (e.g. Terzan 5 with VLT/MAD; Ferraro et al. 2009). However, infrared wavelengths are not typically ideal, by themselves, for detailed studies of resolved stellar populations, unless the population is behind significant foreground dust extinction, like Terzan 5.

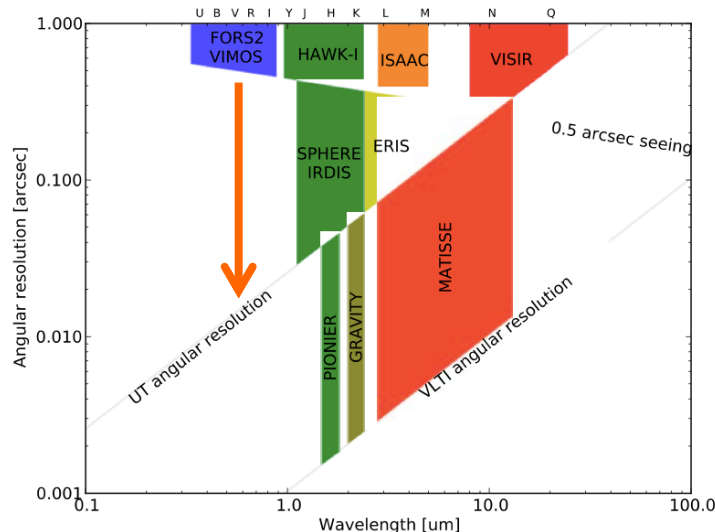
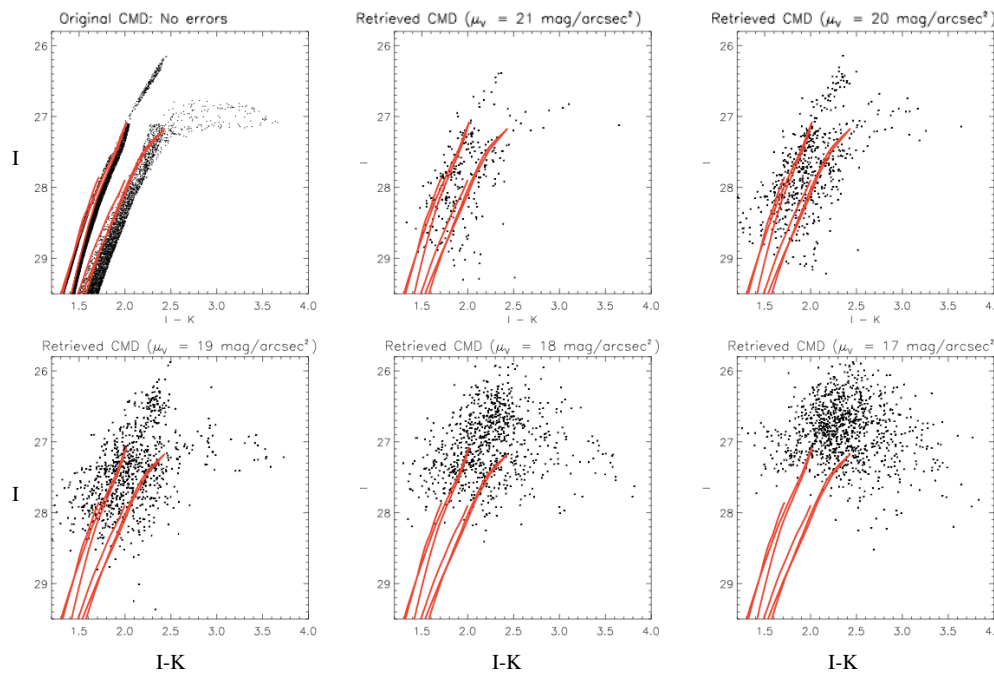


Figure 8: *Wavelength-angular resolution diagram for 1<sup>st</sup> and 2<sup>nd</sup> generation VLT/I instruments at ESO. The large orange arrow shows the potential for improvement in optical wavelengths, between 0.5arcsec (excellent) seeing limit and the diffraction limit of one of the 8.2m UTs. Adapted from ESO/Cou-1681 document.*

The increased spatial resolution, approaching the optical diffraction limit of a VLT UT, needs to be possible over a sufficiently large fraction of the sky. The sensitivity and diffraction limited capabilities need to go down at least to the V-band, and to cover a useful field of view to ensure that resolved stars can be detected and photometered in sufficient numbers of allow an accurate statistical analysis of a CMD and for a reasonable fraction of a galaxy or galactic component. These key requirements for an instrument suitable for resolved stellar population studies are discussed in more detail below.

### 3.1.3.1 Spatial Resolution:

A new optical AO imager needs to achieve at least close to diffraction limited observations with the VLT. This would provide a dramatic increase compared to the current, seeing limited performance, see Figure 8, where it is clear that at optical wavelengths there is significant potential for improvement to match the theoretical limits of the telescope. Increasing the spatial resolution increases the sensitivity in crowded regions by limiting the background from unresolved stars, and enabling images of the individual stars to be accurately measured to fainter limits (e.g. Deep et al. 2011), see Figures 6 and 9. Higher surface brightness obviously corresponds to more stars per square arcsec, so spatial resolution requirements are directly related to surface brightness in a weakly distance dependent way. Figure 9 shows how the sensitivity limit and the accuracy of the photometry change as the surface brightness increases (and so the image crowding increases). This is an example of a simulation for MICADO taken from Deep et al. (2011), but the principle remains the same, with perhaps a small shift in pixel size. MICADO is not optimised for optical wavelengths and so has extremely low performance at its bluest wavelengths, which is an I filter truncated at 800nm.



**Figure 9:** The  $(I, I-K)$  CMDs obtained from simulated MICADO/MAORY images, assuming one hour exposure times, for 5 different surface brightness ( $\mu_V$ ) levels. In the top left hand corner is the original input CMD, without any errors. Included on each panel are the isochrones that represent the mean properties of each distinct stellar population. The highest surface brightness ( $\mu_V = 17 \text{ mag/arcsec}^2$ ) is equivalent to a distance of  $\sim 5 \text{ arcsec}$  from the centre of a typical elliptical galaxy in Virgo (e.g., NGC 4472), whereas the lowest ( $\mu_V = 21 \text{ mag/arcsec}^2$ ) is at a distance of  $\sim 75 \text{ arcsec}$  from the centre. Taken from Deep et al. (2011).

A practical example of the effects of crowding from the literature, is resolved HST imaging of the Sculptor group galaxy NGC253, see Figure 10. The HST/ACS GHOSTS survey fields are shown (from Radburn-Smith et al. 2011), for the 3 arcmin square ACS field of view over the whole galaxy. The CMDs for these images show the increasing effect of crowding for the fields closer to the centre of the disk. Fields 1-4, in Figure 10 are clearly very crowded and the photometry is not optimal, as can be seen from the large amount of scatter. This is where a higher spatial resolution is needed to obtain a reliable quantitative analysis of the CMD in terms of a star formation history. Also the exposure times ( $\sim 30\text{min}$  per filter) are not sufficient to detect the main sequence in this galaxy, however given how crowded these images are, going another 3 magnitudes deeper is not feasible. The only reliable way to correct for these effects of crowding is to observe at higher spatial resolution. HST lacks both the sensitivity and the required spatial resolution to look close to the central disk or bulge of external galaxies, where most of the stars are to be found. HST and indeed seeing limited 8m telescopes are well suited to observe the relatively sparse halo of galaxies like NGC253, but cannot obtain reliable photometry in the more central much more crowded regions where most of the stars are to be found, in the disk and bulge of the galaxy. The diffraction-limited resolution of an 8-m telescope at 450nm matches that of 39m E-ELT at  $2.2\mu\text{m}$  (see Figure 11), and so the combination of MICADO/MAORY on the E-ELT and an optical AO-imager on VLT becomes very powerful to obtain optical and near-infrared



images at matching spatial resolution. Studies in the disk region of highly inclined galaxies like NGC253 will clearly benefit from both optical and infrared observations and are thus excellent targets for synergy with MICADO on the E-ELT, see sections 2.1 & 2.2.

### 3.1.3.2 Sensitivity:

An optical-AO instrument on the VLT has to be efficient enough to guarantee sensitivity gains to match the increased spatial resolution. This sensitivity limit determines the distance and the accuracy possible for CMD analysis (see Figure 2). The increased spatial resolution will naturally ensure that denser stellar fields can be probed, but without suitable sensitivity the fainter stars will not be detected. There remains benefit in only a resolution gain, but the instrument will be more powerful the higher is the throughput. Key numbers are V~29-30 for diffraction limited V-band imaging of the main sequence turnoff region in the optical in the Sculptor group. If this can be pushed even deeper (V~31) than the resolved stellar populations of “normal” elliptical galaxies in the Virgo cluster become accessible as well (see section 2.3). This would be a dramatic improvement on what is currently possible and would support the ambitious goals of MICADO on the E-ELT. However to achieve this it is imperative that an optical-AO instrument is stable enough to allow long exposures, or at least the build up of exposures to increase sensitivity. The advantage of optical imaging is that the background noise level is lower and so the saturation time of the CCD will be longer, potentially making it more efficient to be able to carry out deep exposures. This is highlighted by the HST sensitivity limits plotted in Figure 3.

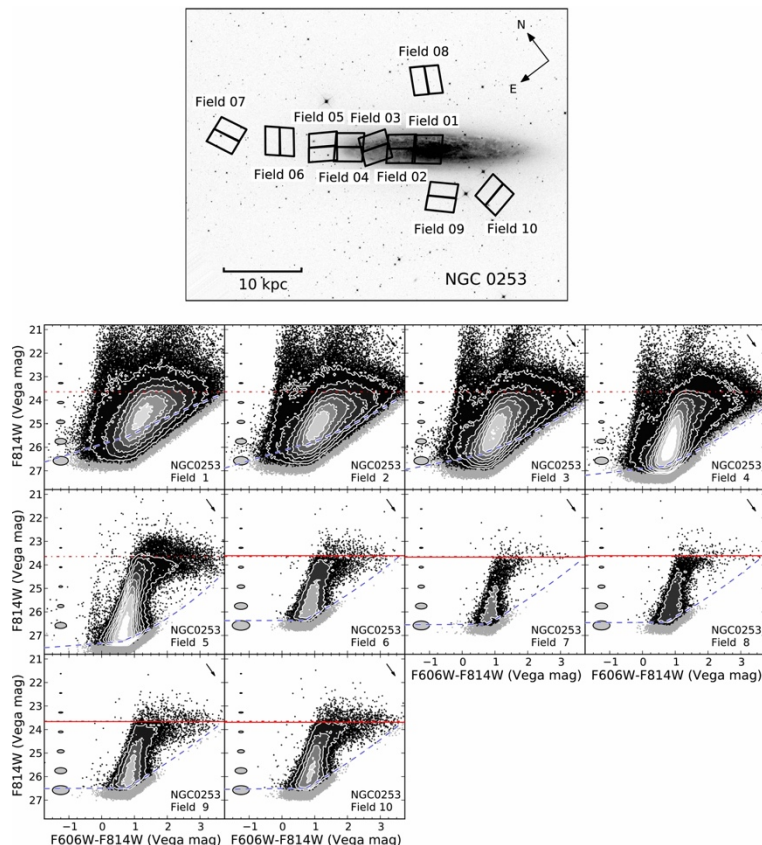


**Figure 10:** Fields observed in NGC253 with HST/ACS. Each field is 3 arcmin square and the observations are around 30mins in each filter ( $F606W \sim V$ ;  $F814W \sim I$ ). The resulting CMDs are shown for each field. Points in grey have the same selection criteria but a lower S/N cut. Shaded ellipses indicate the average  $1\sigma$  photometric uncertainties. The red line is the tip of the red giant branch. The blue dashed line denotes the 20% completeness limit. The direction of reddening, due to foreground Galactic extinction, is indicated by the arrow in each CMD. From Radburn-Smith et al. (2011).

Making estimates of the expected sensitivities of an optical AO camera by scaling the results of the FORS2 ETC to smaller pixels on the same telescope suggests that this kind of magnitude limit should be feasible, although the deepest limit ( $V \sim 31$ ) will be extremely challenging.

### 3.1.3.3 Filters:

The standard filters for classical CMD analysis are B, V and I optical filters, which nicely cover the peak in the spectral energy distribution of most stars. However the most popular combination for HST has actually been V-I, and this is excellent for older stellar systems. For the systems with young stellar populations (such as are shown in Figure 2) the B filter is useful for spreading out and thus separating the younger stellar populations for more accurate analysis. However, the more red older populations are always the faintest and the most crowded, so this is optimum population to aim for improvements from a ground based optical-AO system. The ideal filter combination is actually optical and infrared (see Figure 3). Thus making the synergy between this optical-AO imager and MICADO/MAORY on the

E-ELT an important science driver. However it should also be noted, that in Figure 3, even though the I, V-I CMD is not as spread out as the K, V-K CMD, the photometric errors will be much smaller throughout the CMDs, due to the smaller sky background at optical wavelengths and resulting potential for much deeper photometry. It should be easily possible to detect the oldest Main Sequence Turnoffs in I, V-I, unlike in K, V-K. The synergy between optical and infrared observations will be very important. To match the potential depth and resolution of optical CMDs from a diffraction limited VLT, a much larger telescope is needed. This makes it clear why a VLT diffraction limited telescope in the optical is a good match to E-ELT in the infrared. It should also be noted that MICADO will not have a standard I-filter, as the sensitivity cuts off at 800nm, and the imaging performance at these wavelengths will likely be very poor.

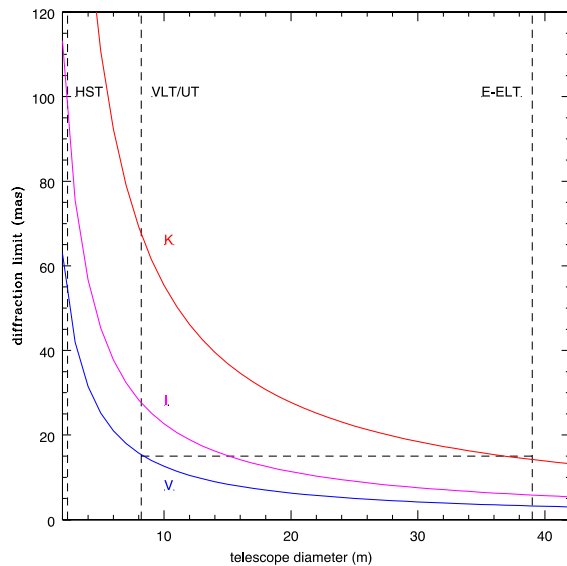


**Figure 11:** The theoretical diffraction limit for three different filters (V, I & K) in relation to telescope diameter. The diameter of HST, VLT/UT and E-ELT are also marked. The horizontal dashed line shows the equivalence of the diffraction limit of a VLT/UT in the V-band to a 39m E-ELT in the K-band.

### 3.1.3.4 The Field of View:

The ideal field of view is of course as large as possible. The most crowded regions in external galaxies in the nearby Universe decrease in size with distance, or are sufficiently dense that statistics to sample the stellar population of a particular component can be achieved with a relatively small field of view (see sections 2.1 & 2.2). Being able to match the MICADO high-resolution field of view is a key point. So, the field of view should be at least 20 arcsec square.

A range of different galaxies, visible in the southern hemisphere, that are of potential interest to study their resolved stellar population are listed in Table 1. The sizes of several of these galaxies are very large, compared to the likely field of view of an optical AO imager on the VLT (or MICADO), but the individual components where crowding is the most extreme, like the central regions, the bulge, the spiral arms, can be studied in smaller regions. These are at sufficiently high surface brightness to require the resolution of the diffraction limited optical AO, and thus also to populate a CMD with a statistically significant number of stars to ensure a useful analysis of the stellar properties.



D (Mpc)		oMST OM <sub>I</sub> = -3	TRG B M <sub>I</sub> =4	M <sub>V</sub>	Major d (arcmin)	Minor d (arcmin)	Notes
WLM	1	28	21	-14.8	11.5	4	IB(s)m
NGC3109	1.3	28.6	21.6	-16.1	19.1	3.7	SB(s)m
NGC55	1.9	29.4	22.4	-19.3	32.4	5.6	SB(s)m
NGC300	1.9	29.4	22.4	-19	21.9	15.5	SA(s)d
NGC247	3.2	30.7	23.7	-19.8	21.4	6.9	SAB(s)d
NGC253	3.2	30.7	23.7	-22	27.5	6.8	SAB(s)c; Starburst
NGC7793	3.8	31	24	-20	9.3	6.3	SA(s)d
CenA	3.8	31	24	-21.4	25.7	20	S0 pec;Sy2 BLLAC
NGC1705	5	31.5	24.5	-18	1.9	1.4	SA0- pec: BCD
M83	6.5	32	25	-21.5	12.9	11.5	SAB(s)c; Starburst
M104	11.3	33.3	26.3	-22.7	8.7	3.5	SA(s)a; Sy1.9
NGC1068	12.5	33.5	26.5	-22	7.1	6	(R)SA(rs)b; Seyfert
M59	15.5	33.9	26.9	-22.8	5.4	3.7	E5 AGN
M49	15.8	34	27	-24.2	10.2	8.3	E2
M86	16	34	27	-24	8.9	5.8	S0/E3
M89	16	34	27	-22.6	5.1	4.7	E/Sy2
NGC4478	16.1	34	27	-20.5	1.9	1.6	E2
NGC4550	16.2	34	27	-20.3	2.5	0.8	SB0
M87	16.5	34	27	-23.9	8.3	6.6	E+0-1 pec
M60	16.6	34	27	-23.6	7.4	6	E2
NGC4342	16.8	34.1	27.1	-20	1.3	0.6	SO-
M84	16.8	34.1	27.1	-25	6.5	5.6	E1; Sy2
NGC4623	16.8	34.1	27.1	-19.6	2.2	0.7	SB0+
NGC4564	16.9	34.1	27.1	-21	3.5	1.5	E6
NGC4570	17.6	34.2	27.2	-21	3.8	1.1	S0/E7
NGC1399	19.0	34.4	27.4	-23	6.9	6.5	E1 pec Sey2
NGC1404	19.0	34.4	27.4	-22.4	3.0	3.0	E1

**Table 1:** A selection of nearby galaxies where the resolved stellar populations are potential targets for an optical AO imager on the VLT, and also for combined infrared observations with MICADO on the E-ELT.

### 3.1.3.5 Sky coverage:

Another important aspect of an optical AO imager on the VLT is that the majority of galaxies that would be targeted do not have conveniently placed bright nearby guide stars. These are rare over the relatively small fields of view being contemplated here. These science cases would be adversely affected by severe restrictions in positioning the field of view. Also the MUSE NFM will need a bright (<15 mag) central TT-source within the 7.7"x7.5" field of view thus limiting severely the sky coverage. For example the Gemini/Altair data shown in Figure 5 used a globular cluster as a Guide star, and of course this biases the information about the stellar population in this area in such away that could easily affect the scientific interpretation of the results. This means a more creative solution is absolutely required to be able to observe these systems with a suitably high AO performance in the optical (or infrared) for something close to all sky coverage.



### 3.1.3.6 Image stability

Proper motion measurements require exquisite accuracy in determining positions of stars within images taken over many years (see Figure 7), see Section 2.4. To obtain a measure of how much stars will move over this time scale requires the ability to distinguish instrumental effects from true motion on the smallest of (sub-pixel) scales. The more accurately the positions can be measured the more accurate and quick can be proper motion measurements. The higher the spatial resolution of an instrument, and the more stable it is the better it is for astrometry. Image stability is also important for enabling the efficient build-up of long integrations to create deep images of distant systems.

### 3.1.4 Summary

It is clear that there are major technical challenges to overcome before an optical AO instrument useful for studying resolved stellar populations can be realised. SPHERE/ZIMPOL and the GeMS/GMOS experiment have shown that optical AO is feasible. This now needs to be developed and extended for a larger field of view and for more extensive sky coverage. The system also needs to be stable to be able to make long exposures and build up the sensitivity of individual images. The rewards for overcoming these difficulties will be a breakthrough in our understanding of the role of the Milky Way and its satellites as a template for galaxy evolution by comparing its properties, which will be exquisitely defined when the final Gaia catalogues are released, to those of a range of different spiral galaxies beyond the Local Group. We will also be able to understand the role of bulge growth in a range of different galaxy types to explain the diversity of properties in different types of galaxies. We should also come a big step closer to carefully disentangling the resolved stellar populations that make up normal elliptical galaxies and have a detailed tie in to high redshift studies probing the formation of these large stellar systems.

## **Bibliography:**

- Aloisi A. et al. 2007** ApJL, 667, 151 *I Zw 18 Revisited with HST ACS and Cepheids: New Distance and Age*
- Baade W. 1944a** ApJ, 100, 137 *The Resolution of Messier 32, NGC 205, and the Central Region of the Andromeda Nebula*
- Baade W. 1944b** ApJ, 100, 147 *NGC 147 and NGC 185, Two New Members of the Local Group of Galaxies*
- Bellini A. et al. 2014** ApJ, 797, 115 *Hubble Space Telescope Proper Motion (HSTPROMO) Catalogs of Galactic Globular Clusters. I. Sample Selection, Data Reduction, and NGC 7078 Results*
- Belokurov V. & Koposov S.E. 2015** MNRAS, 456, 602 *Stellar streams around the Magellanic Clouds*
- Bernard E. et al. 2015** MNRAS, 453, L113 *The spatially-resolved star formation history of the M31 outer disc*
- Cignoni M. & Tosi M. 2010** Adv. Astron., *Star Formation Histories of Dwarf Galaxies from the Colour-Magnitude Diagrams of Their Resolved Stellar Populations*
- Cignoni M. et al. 2012** ApJ, 754, 130 *Star Formation History in Two Fields of the Small Magellanic Cloud Bar*
- Cole A.A. et al. 2007** ApJL, 659, L17 *Leo A: A Late-blooming Survivor of the Epoch of Reionization in the Local Group*
- Davidge T. et al. 2005** AJ, 129, 201 *Deep ALTAIR+NIRI Imaging of the Disk and Bulge of M31*
- Davies, R. I. & Kasper M. 2012** ARAA, 50, 305 *Adaptive Optics for Astronomy*



- Davies, R. I. et al. 2015** ESO in the 2020s, Garching, Germany *Resolved Stellar Populations with Visible Adaptive Optics on the VLT*  
[https://www.eso.org/sci/meetings/2015/eso-2020/Davies\\_ESOin2020s.pdf](https://www.eso.org/sci/meetings/2015/eso-2020/Davies_ESOin2020s.pdf)
- Deep A. et al. 2011** A&A, 531, A151 *An E-ELT case study: CMDs of an old galaxy in the Virgo cluster*
- Durrell P.R. et al. 2007** ApJ, 656, 746 *The Resolved Stellar Populations of a dSphl Galaxy in the Virgo Cluster*
- Esposito S. et al. 2016** Proc. SPIE, 9909, id. 99093U *AOF upgrade for VLT UT4: an 8m class HST from ground*
- Ferraro F. et al. 2009** Nature, 462, 483 *The cluster Terzan 5 as a remnant of a primordial building block of the Galactic bulge*
- Geha M. et al. 2015** ApJ, 811, 114 *HST/ACS Direct Ages of the Dwarf Elliptical Galaxies NGC 147 and NGC 185*
- Genzel R., Eisenhauer F. & Gillessen S. 2010** Rev. Mod. Phys., 82, 3121 *The Galactic Center massive black hole and nuclear star cluster*
- Grocholski A.J. et al. 2012** AJ, 143, 117 *HST/ACS Photometry of Old Stars in NGC 1569: The Star Formation History of a nearby Starburst*
- Hubble E.P. 1925** ApJ, 62, 409 NGC 6822, a remote stellar system
- Kormendy J. et al. 2009** ApJS, 182, 216 *Structure and Formation of Elliptical and Spheroidal Galaxies*
- Monachesi A. et al. 2011** ApJ, 727, 55 *The Deepest HST CMD of M32. Evidence for Intermediate-age Populations*
- Olsen K. et al. 2006** AJ, 132, 271 *The Star Formation Histories of the Bulge and Disk of M31 from Resolved Stars in the Near-Infrared*
- Pietrinferni A. 2004** ApJ, 612, 168 *A Large Stellar Evolution Database for Population Synthesis Studies. I. Scaled Solar Models and Isochrones*
- Rejkuba M. et al. 2011** A&A, 526, A23 *How old are the stars in the halo of NGC 5128 (Centaurus A)?*
- Radburn-Smith D.J. et al. 2011** ApJS, 195, 18 *The GHOSTS Survey. I. HST/ACS Data*
- Salaris M. et al. 2013** A&A, 559, A57 *The horizontal branch of the Sculptor dwarf galaxy*
- Simon J.D. & Geha M. 2007** ApJ, 670, 313 *The Kinematics of the Ultra-faint Milky Way Satellites: Solving the Missing Satellite Problem*
- Tolstoy E., Hill V. & Tosi, M. 2009** ARAA, 47, 371 *Star-Formation Histories, Abundances, and Kinematics of Dwarf Galaxies in the Local Group*
- Tolstoy E. 2011** Science, 333, 176 *Galactic Paleontology*
- Weisz D.R. et al. 2014** ApJ, 789, 147 *The Star Formation Histories of Local Group Dwarf Galaxies. I. Hubble Space Telescope/Wide Field Planetary Camera 2 Observations*



## 3.2 Solar System Science and Outreach

By Olivier Hainaut, ESO, Garching bei München, Germany

Note: this section deals *only* with *our* solar system. The cases for exo-solar-systems are not included.

### 3.2.1 Planets

#### 3.2.1.1 Planetary weather reports

While in-situ observations of the planets are hard to beat in terms of resolution, remote ground-based high-resolution imaging allows us to monitor the planets' atmospheres over long time. The Great Red Spot on Jupiter, the (ir-)regularly occurring Great White Spots on Saturn, the usually almost featureless atmosphere of Uranus and the complex but extremely poorly documented atmosphere of Neptune have benefitted from such monitoring with Hubble over the past two decades. A continuation at 3x the resolution of Hubble (see table 1) will continue to bring information on these atmospheres, at a time when comparison with giant exoplanets will make comparative planetology possible.

With a FoV of 40 - 60arcsec covers the disc of most planets over most of their orbit (Jupiter can cover almost 1 arcmin when at its best geometry). A monitoring program of the giant planets will bring the study of their atmosphere into the realm of geophysics and climate science, which is impossible with an occasional snapshot.

Table 1: number of resolution elements across the planets' diameter using visible AO on a UT

Planet	Number of resolution elements
Jupiter	Up to 2900 (the planet just fills the FoV)
Saturn	>1000
Uranus	240
Neptune	150

#### 3.2.1.2 Large satellites

Again, it is not (yet) possible to beat the resolution of in-situ observations of the large planets' satellites. Nevertheless, many of them display time variability caused by a variety of phenomena: complex atmosphere (in the case of Titan), tidal-stress induced volcanism (Io, which also features a plasma torus connecting it to Jupiter's magnetic field) or cryovolcanism (Enceladus). The understanding of these processes would greatly benefit from being studied regularly. While IR imaging and spectroscopy are helpful in the case of the (hot) Io, the higher resolution in the visible and better sensitivity in the visible are advantageous to study phenomena that appear best in reflected sunlight.



[caveat: except Io's torus, the objects are a few arcsec in diameter; B-I range perfect for spectroscopy; resolution should be at least 5000; 10k is OK, as the surface brightness of the objects is high flux is not an issue]

### 3.2.1.3 Solar System RRM

Furthermore, countless amateurs using fast detectors on fairly large telescopes provide the community with an almost continuous monitoring of the planets with a resolution of a few arcsec. Rapid response observations at high-resolution following-up the transient phenomena detected by these amateurs will be made possible by a visible AO system on the VLT. Except for the case of Mars (with its quasi-continuous fleet of local satellites orbiting the planet), these high-resolution observations will provide a new look at the phenomena taking place in the planets' atmospheres.

### 3.2.2 Cometary activity

Most cometary nuclei are too small to be resolved from the ground. Cometary activity, however, is normally originating from discrete area on the surface, which produce features observable from the ground. These jets and fans turn on and off following diurnal and seasonal cycles. While they can often be observed with seeing-limited images, tracking them down as close to the nucleus as possible is critical for their proper interpretation, which results in a full model of the active areas on the nucleus. Except for the handful of comets that were visited by spacecrafts, these reconstructions are the best information available. The dust jets and fans are best observed in the V and R bands<sup>1</sup>, so a visible AO system on the VLT would be *the* instrument of choice. The current state-of-the-art is illustrated in Figure 1.

Furthermore, a set of narrow-band filters (centered on cometary line features, e.g. the "Hale-Bopp Filter Set"<sup>2</sup>) would also be advantageous to track the spatial distribution of the most important cometary species in the near-nucleus coma, and back to the nucleus. The angular resolution of the VLT combined with its large collecting area will give a great advantage to this field.

[caveat: the most interesting lines would be OH at 305nm and CN at 388nm]

The most interesting objects will be nearby, and therefore rather bright<sup>3</sup>. S/N is therefore not the limiting factor; spatial resolution is. A ~1arcmin FoV with high-resolution ensures a robust connection between the high-resolution near-nucleus features and their broad extension (from 1 to 10arcmin for normal comets, to 100arcmin for bright nearby objects).

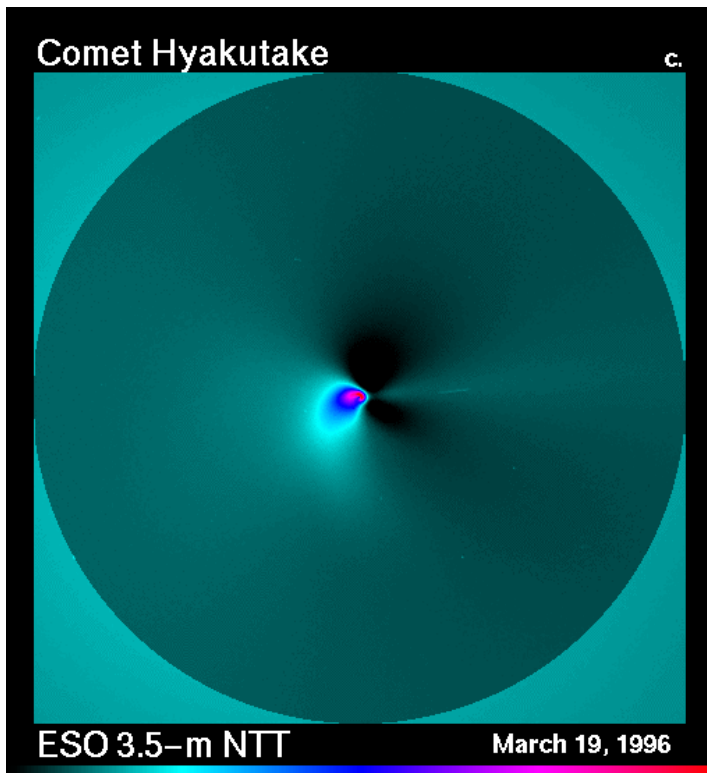


Figure 1 -- Inner coma of nearby bright comet Hyakutake. The cometary features in this 1arcmin FoV have been enhanced by removing an average profile of the object. The broad fan (on the left) can be tracked spiraling down to the nucleus, where it lost in the (0.6") seeing blob. Credit: ESO.

[source: <http://www.eso.org/public/images/eso9623c/> ]

### 3.2.3 Deep photometric observations

The size distribution of trans-Neptunian objects (TNOs) has been characterized using the population discovered in wide-field surveys, and extended to the faint-end using narrow “pencil-beam” surveys. A break in the size distribution is inferred and --at least partly-- confirmed observationally, whose position corresponds to a change of scale in the accretion and ablation processes forming these minor planets.

On the other hand, the surface characterization of the many dynamical classes of TNOs has been limited to by the small size of most objects, their distance from the Sun, and the limiting magnitude of the instruments. The bulk of the measurements is on objects brighter than  $V=23$ , with some projects pushing the limit to 25 on a smaller number of objects. The fairly simple and featureless spectra of these objects are well characterized with BVRIJ photometry. The fainter limiting magnitudes<sup>4</sup> made possible by a visible AO system would allow us to extend the surface studies at and beyond the size distribution break-point. This would in turn allow modelers to disentangle formation, migration and evolution processes.

[caveat: for this science case, FoV is not relevant. Spectral resolution >100 is not relevant]



### 3.2.4 Small satellites

The inventory of small satellites around the 4 giant planets was completed from serendipitous discoveries by in-situ spacecrafsts, but mostly using wide field imagers. It reaches 50% completeness around mag 26. A small niche could be explored with the VLT, searching for very small satellites in the immediate surroundings of the planet i.e. where the glare of the planet blinds wide-field imagers, and where a diffraction-limited images would allow deeper magnitudes to be reached.

The orbits of the spacecrafsts are optimized for the planets and the main satellites. For many of the small satellite, only their orbit and very basic parameters are known either from some spacecrafst observations or from the ground. Ground-based AO could provide their (integrated) surface properties, from which their origin and formation can be inferred.

[caveat: the large FoV is not needed; optimal spectral resolution: few thousands]

### 3.2.5 Rings

The four giant planets are known to harbour ring systems of various structural complexities. The large collecting area of the VLT combined with the resolution of the AO system will be significantly more efficient than HST to detect and characterize the very low surface brightness rings. In many cases, their shepherd satellites are either not known or not studied --this can be done with a visible AO on the VLT.

Recently, ring systems have also been discovered around icy minor planets. Their distance (typically beyond Saturn) and small size (few hundred km diameter) make for challenging observations: Chariklo's rings would be covered by 4 resolution elements (see Figure 2).

[caveat: nIR xAO might be better than VisAO for these objects; FoV is not relevant; spectroscopy marginally relevant]



*Figure 2 - A photometrically and geometrically correct artist view of distant icy minor planet Chariklo. The field of view of this image would be 6 resolution elements of VAOI system, i.e. the rings would be detectable. Wider and/or closer objects would be more easily measured. Credit: ESO/L. Calçada/M. Kornmesser/Nick Risinger (skysurvey.org) [source: <http://www.eso.org/public/images/eso1410b/> ]*

### 3.2.6 Outreach

The production of outreach images is a requirement for a large observatory. It is *the* product that can make an astronomical facility known to the public, and attract a general audience to more advanced scientific results.

The production of outreach-quality images is a valuable add-on for this instrument. The main parameters defining the quality of an image for outreach purposes are:

- The “photogenic resolution” of the image, that is the number of resolution elements across the FoV. Values above 1000 result in stunning images (VST is >4000, HST > 2000); above 200-300 in acceptable images (FORS can reach 400 in good conditions), and images with a value below 100 are barely acceptable (they look fuzzy, no matter what the actual angular resolution is). This is why very few NaCo images resulted in good images for outreach purposes.  
This new instrument, with a 30-50" FoV and a resolution element of 17mas leads to “photogenic resolution” of 1500 to 3000, i.e. excellent.
- Colours: a combination of broad-band and narrow-band filters (ideally 3-5 filters) covering a range of astrophysical phenomena (e.g. sampling the SED of the objects, plus some interesting emission lines) fill the colour space of the final image. While ~monochrome objects can look interesting, colours tend to make better looking outreach images. In the Near-IR range, the very small dispersion of stellar colours tend to make all stellar system whitish. In the visible, the broad



range of stellar colours tend to lead to more interesting images. H $\alpha$  and the various nebular lines (chiefly OIII) give very nice contrasts.

The new instrument, with VRI filters and corresponding narrow bands, will give very interesting combinations.

- Dynamic range: the data used to produce outreach images must have a very broad dynamic range, with some “shallow” exposures showing the brightest sources unsaturated, and some deep and very deep exposures capturing the faint surface brightness features.  
The new AO instrument can take series of exposures over a broad range of exposure times.
- Target: while the artistic composition of an outreach image plays a role in its final appeal, the target is critical. It should nicely fill the FoV. While the number of targets for a wide-field instrument (like VST or WIFI) is limited (and most of them have been imaged over and over), a small FoV combined with high-resolution has a virtually endless list of potentially good-looking targets:
  - Many ~distant galaxies, with the whole bestiary of interacting galaxies (e.g. Arp catalogue);
  - Many galactic planetary nebulae (with their whole range of morphologies);
  - While extragalactic clusters constitute the target of choice of Hubble (in particular through its various ultra-deep legacy projects),
  - A nearly infinite set of “details” in large objects. While the whole object has been photographed over and over, a 17mas resolution reveals many nice features.

Currently, a very successful “filler program” has been running on FORS - the ESO Cosmic Gems project - using a combination of constraints parameters that is useless for most science programs (e.g. good seeing with clouds and moon). However, because of the limitation of FORS (esp. in terms of its “photogenic resolution”), this program is now scraping the bottom of the barrel of nice objects.

A similar program could be implemented on the proposed visible AO instrument, providing an endless stream of original, top quality outreach images.

Overall, a 30-50” FoV diffraction-limited imager would allow ESO to continue its production of top quality outreach images.



*Figure 3 - This FORS image has a similar photogenic resolution as a VisAO system on VLT. The dark globules are examples of objects that would nicely fill the VisAO FoV. This outreach image was produced in the framework of the “ESO Cosmic Gems” filler program that is executed only when the conditions are unusable by any science program. Credit: ESO*

[source: <http://www.eso.org/public/images/eso1322a/> ]



### 3.3 Giant star-forming clumps at high redshift: the new viewpoint offered by visible AO on VLT

By Anita Zanella, ESO, Garching bei München, Germany

#### Abstract

Spatially resolving high-redshift galaxies is one of the most promising way to understand their structure and evolution. While local sources typically have low star formation rates and exhibit regular (spiral-like or bulge-dominated) structures, the majority of galaxies at high redshift ( $z \sim 1 - 2$ ) seem to be actively star-forming and show irregular morphologies. They are dominated by bright patches with blue colors (dubbed “clumps”) standing out of the underlying disk. Clumps have typical sizes  $\leq 1$  kpc ( $\leq 0.1''$  at  $z \sim 2$ ), stellar masses  $\sim 10^9 M_{\odot}$ , and are actively star forming. They have been discovered thanks to the high spatial resolution and flux sensitivity of the *Hubble Space Telescope*, but despite being known since a while, their origin, fate, and properties are still highly uncertain. In particular, their contribution to galaxy evolution is widely debated: it is not clear if, migrating toward the nucleus of the disk during their lifetime, they can contribute to the growth of the bulge and the fuelling of the central supermassive black hole. This could help explaining the morphological evolution of galaxies observed through cosmic time. Furthermore, it is not clear yet if clumps form in-situ due to the fragmentation of gas-rich disks or if they have an ex-situ origin and merge with galaxies. Disentangling the two scenarios could help to understand the physical conditions of the gas in high-redshift sources and to put constraints on the different scenarios proposed for galaxies mass assembly (e.g. cold gas replenishment smoothly flowing from the cosmic web or merger episodes?). Finally, the properties of the clumps themselves (their sizes, masses, gas condition, initial mass function...) are still little constrained and heavily affected by blurring and dimming. An optical instrument on VLT with diffraction-limited spatial resolution, high flux sensitivity, and a relatively large field of view ( $30'' - 40''$ ) would be particularly suitable to study samples of clumps. These observations could substantially broaden the parameter space currently explored and would complement the data taken by E-ELT/HARMONI at near-infrared wavelengths, allowing us to reach a multiwavelength and comprehensive view of galaxies down to kpc-scales.

#### 3.3.1 Introduction

Galaxies are usually considered to be the fundamental building blocks of the Universe. Nevertheless, their formation is still observationally poorly constrained and only in a relatively recent epoch it has been understood that they evolve as time passes. This discovery has mainly been possible thanks to the advent of the *Hubble Space Telescope* (*HST*): it clearly showed that distant galaxies have different morphologies and physical properties with respect to local ones, suggesting a progression from high-redshift sources – that are mainly small, peculiar, and highly star-forming – to the relatively quiescent ones found locally (Conselice 2014 and references therein). A consistent picture is emerging, indicating that the

Universe was much more active in the past, where stars formed at a rate almost ten times higher than today. The star formation rate (SFR) density appears to peak approximately 3.5 Gyr after the Big Bang, at redshift  $z \sim 2$ , dropping exponentially at  $z < 1$  (Figure 1, Madau & Dickinson 2014), and almost 50% of the present-day stellar mass density was formed at redshift  $1 \leq z \leq 3$ . It is therefore crucial to directly study this redshift range to understand what were the driving forces creating galaxies and which are the physical processes that brought to the build-up of their mass. In particular, it is critical to study distant galaxies with the same spatial detail achievable in the local Universe to finally pinpoint what are the reasons why high-redshift sources are intrinsically different from local ones, and to understand how galaxies evolution took place through cosmic time.

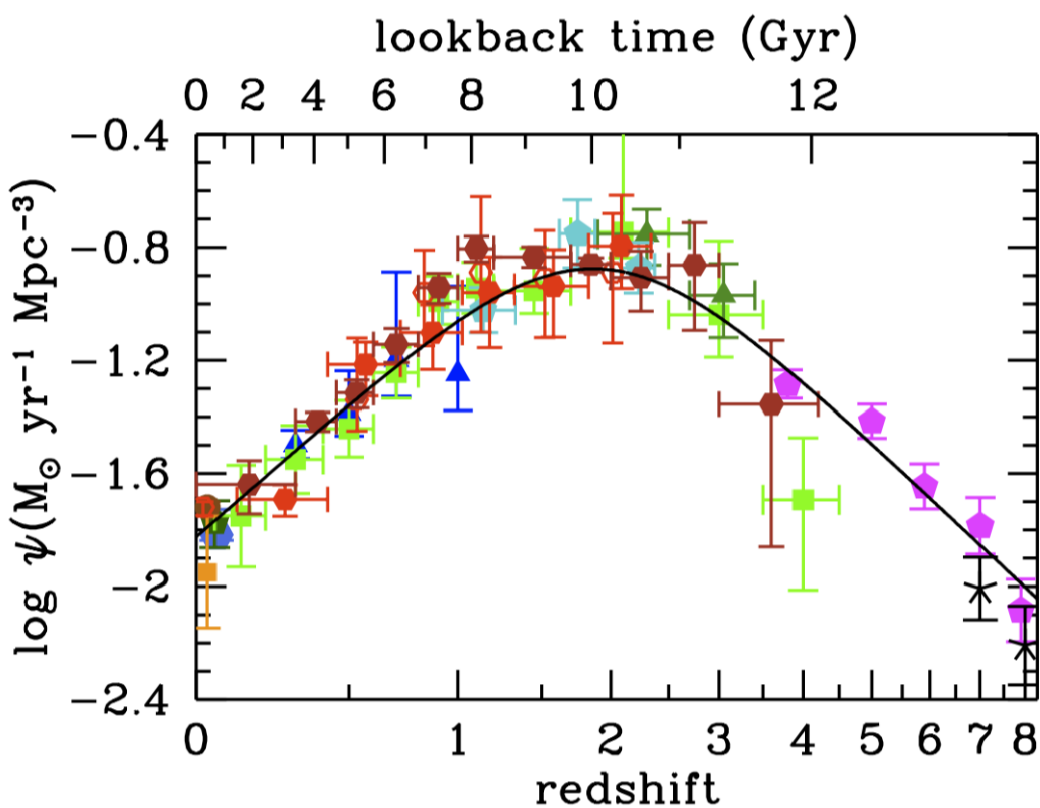


**Figure 1: The history of cosmic star formation from far-ultraviolet and infrared measurements. Different symbols represent distinct datasets (Madau & Dickinson 2014).**

The first attempts to study galaxies structure down to kpc scales at high redshift has been possible thanks to the high spatial resolution of *HST* and the depth of its observations. As initially seen in the Hubble Deep Field (Abraham et al. 1996; van den Bergh et al. 1996; Cowie et al. 1996), the majority of galaxies at  $z \geq 2$  have an irregular morphology, dominated by bright patches on top of a diffuse emission. Before *HST* observations, these kind of peculiar structures were usually observed in nearby dwarf galaxies. However, the irregular sources detected at high redshift are 10 – 100 times more massive, a mass regime where local galaxies are mostly regular disks or spheroid-dominated early type galaxies. Thanks to spatially-resolved stellar population studies it has been found that the bright patches clearly visible in optical observations were not just transient associations of bright stars, but they



were massive clumps with sizes of  $\leq 1000$  pc, stellar masses of  $\sim 10^9 M_{\text{sun}}$ , and stellar ages typically younger than the host galaxy (Elmegreen & Elmegreen 2005; Guo et al. 2012; Wuyts et al. 2012). These structures are generally dubbed “giant clumps”, and their hosts “clumpy galaxies”.

Giant clumps are mostly identified in deep and high-resolution rest-frame ultraviolet (UV) and optical images (e.g. Elmegreen et al. 2009; Förster Schreiber et al. 2011; Guo et al. 2015), but they are also observed in rest-frame optical line emission from spatially-resolved, near-infrared (NIR) spectroscopy (e.g. Genzel et al. 2008; Genzel et al. 2011; Zanella et al. 2015) and CO line emission of lensed galaxies (e.g. Jones et al. 2010; Swinbank et al. 2010). They have blue colors and enhanced specific star formation rate, typically higher than their surroundings by a factor of several (e.g. Guo et al. 2012; Wuyts et al. 2012; Wuyts et al. 2013). Their host galaxies have in great majority disk-like velocity fields, showing the typical signature of rotation, and no signs of on-going or recent major mergers, despite their irregular morphology (Figure 2).

However, studying giant clumps with the currently available ground-based facilities and even with *HST* is still challenging. Very high spatial resolution ( $< 0.1'' - 0.2''$ , corresponding to  $< 1 - 2$  kpc at  $z \sim 2$ ) and flux sensitivity (e.g.,  $V > 27$  AB mag for point sources) are needed in both photometric and spectroscopic data to resolve galaxies and eventually the clumps themselves. Ideally, large fields of view ( $\sim 30''$ ) are also necessary to gather statistically meaningful clumps samples. Therefore, to make a significant step forward toward the understanding of high-redshift star-forming galaxies, it is crucial to get a ground-based instrument performing observations with extreme adaptive optics (AO) correction over a large field of view. Given the high clumps SFR and blue colors, probing the rest-frame UV part of the spectrum is particularly compelling, therefore the need for a facility that can carry out observations in optical bands. Finally, these data could nicely complement the NIR *JWST* /MIRI and *E-ELT/HARMONI* observations (Section 3), hopefully matching their depth and spatial scale, opening the doors to a more complete understanding of high-redshift galaxies.

### 3.3.1.1 Open questions that a new optical instrument could answer

A *VLT* instrument that can deliver diffraction-limited observations in optical bands would allow in the coming years to make considerable steps forward in the understanding of high-redshift clump properties and their impact on galaxy evolution. This is still a relatively new and completely open research domain that we have been able to start exploring only by pushing current instruments to their limits. The study of giant clumps is therefore an optimal science case for new facilities, designed to reach unprecedented flux depth and resolution, that could easily bring to unexpected breakthroughs.

Current *HST* and ground-based, AO-assisted observations of giant clumps at  $z \sim 2$  can be performed with a spatial resolution of  $\geq 1$  kpc down to an emission line flux limit of  $\geq 5 \times 10^{-18} \text{ erg s}^{-1} \text{ cm}^{-2}$  and a continuum AB magnitude of  $\sim 27$ . This only allows us to probe the most massive ( $M_{\text{star}} \geq 10^9 M_{\text{sun}}$ ) and highly star-forming ( $\text{SFR} \geq 10 M_{\text{sun}} \text{ yr}^{-1}$ ) clumps. However, we are likely missing clumps with lower mass, size, and SFR that, according to simulations, should be the majority of the population (Bournaud et al. 2015). Furthermore, there is the possibility that the unresolved blobs that we are studying at high redshift as single objects are in reality clusters of smaller individual clumps, blurred due to the insufficient resolution of the data. This worry is further stoked by the observations of clumps hosted in

local analogs of high-redshift clumpy galaxies (Fisher et al. 2017). These sources have gas fractions, masses, and SFRs comparable to those of  $z \sim 2$  star-forming disks and thanks to their proximity ( $z \leq 0.1$ ) they can be studied with a resolution of  $\sim 100$  pc. These disks seem to fragment and form clumps with average size  $\sim 600$  pc, mass  $M_{\text{star}} \sim 10^8 M_{\text{sun}}$ , and line luminosity  $\sim 5 \times 10^{-19}$  erg s $^{-1}$  cm $^{-2}$ . Similar results have been obtained when looking at high-redshift lensed galaxies, that thanks to magnification allowed to reach analogous depths and resolution (Jones et al. 2010; Swinbank et al. 2010). The effect of surface brightness dimming and blurring with distance is shown in Figure 3, where local clumpy galaxies from the DYNAMO survey have been smoothed to match the flux sensitivity and resolution currently available for  $z \sim 1 - 2$  observations (Fisher et al. 2017)

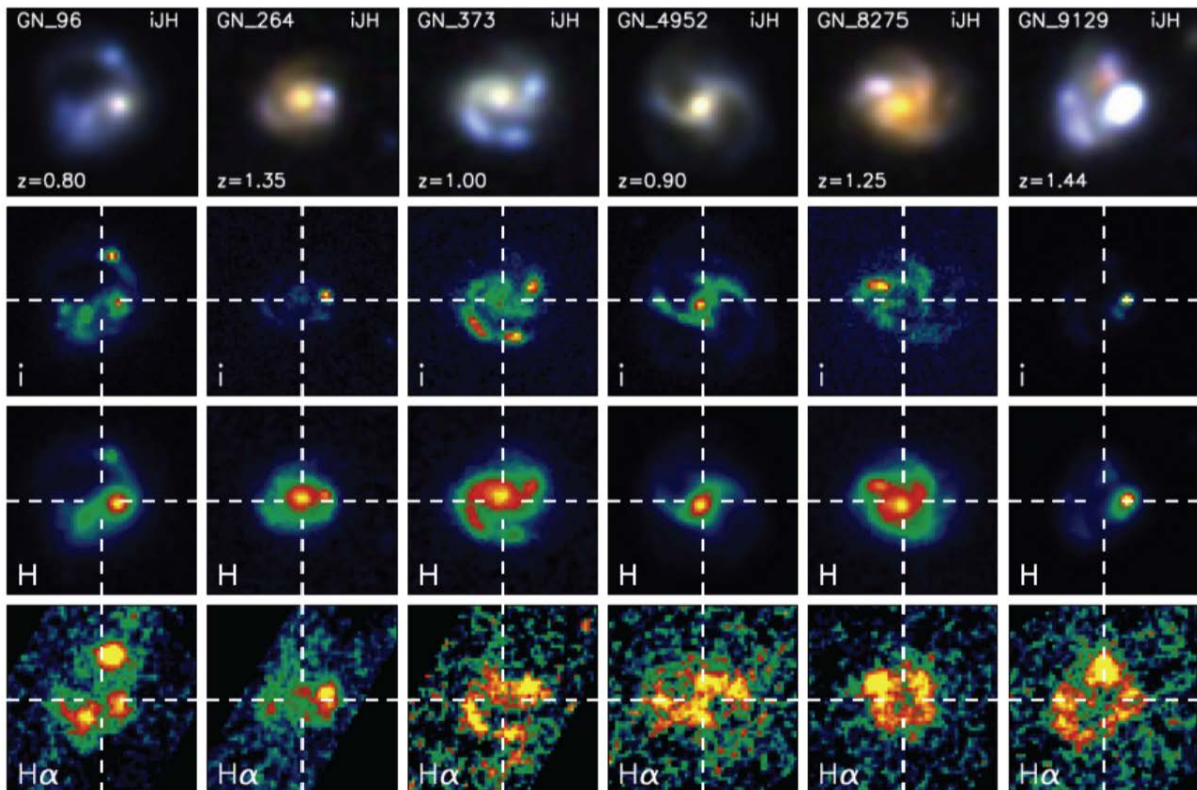


**Figure 2: Examples of massive  $z \sim 1$  star-forming clumpy galaxies. First row: PSF-matched three-color images, sized  $3'' \times 3''$ . Second row: surface brightness distributions in I band. Third row: surface brightness distributions in H band. Fourth row: surface brightness distributions in H $\alpha$  (Wuyts et al. 2013).**

An optical instrument on *VLT* reaching a spatial resolution  $\sim 0.02'' - 0.03''$  (Strehl ratio  $\sim 10\% - 20\%$ ) and an AB magnitude  $\geq 27$  for unresolved sources could allow us to observe  $z \sim 1 - 2$  star-forming galaxies with a similar degree of details available for local sources. This will be of fundamental importance to start making systematic comparisons, understand whether high-redshift clumps are sensibly different from local ones, and infer how their properties possibly evolved with cosmic time influencing (or not) the morphological and structural transformation of the host.

Naturally, by increasing the depth of the observations the galaxy disk becomes brighter and the contrast with the clumps decreases making it more difficult to detect and isolate the star-



forming regions. However, many efforts have been done already with *HST* observations to automatically disentangle the light of the clumps from that of the host: it has been shown that modelling and subtracting the galaxy disk leaves residual maps where the clumps clearly pop up and can be localized (e.g. Guo et al. 2015, Zanella et al. 2015, Cibinel et al. 2017). A similar procedure could be safely adopted also for future instruments.

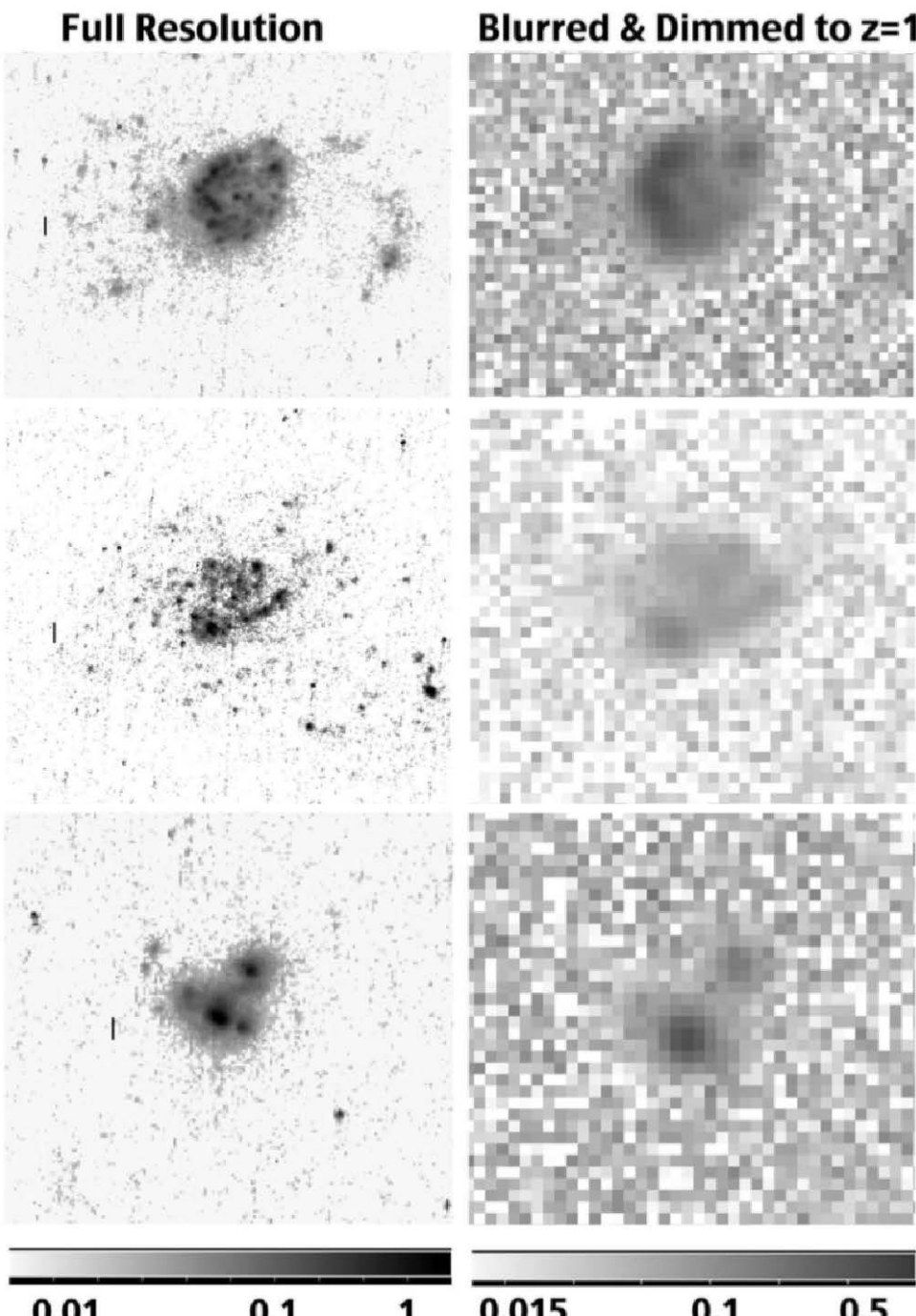


**Figure 2: Comparison of local and high-redshift H $\alpha$  emission line maps.** Left column: H $\alpha$  maps of nearby galaxies ( $z \leq 0.1$ ) from the DYNAMO survey. Right column: DYNAMO H $\alpha$  maps degraded to simulate  $z \sim 1$  observations. Blurring, surface brightness dimming and a sensitivity cut similar to high-redshift AO assisted observations have been applied. The full-width-at-half-maximum of the blurring corresponds to 1.6 kpc and the pixels have a size of 0.8 kpc. The color bar indicates the flux in units of  $10^{-18} \text{ erg s}^{-1} \text{ cm}^{-2} \text{ Å}^{-1}$  and the brightness scale is the same for all maps (Fisher et al. 2017).



In the following we highlight three open questions that a diffraction-limited optical instrument on VLT could answer.

### 3.3.1.2 How are clumps formed?

Although the presence of giant clumps in high-redshift galaxies is known since a while, their real nature and formation process remain still uncertain and debated. Do these clumps form in-situ, as predicted by some high-resolution hydrodynamical and cosmological simulations, due to the fragmentation of gas-rich turbulent disks (e.g. Bournaud et al. 2011, Mandelker et al. 2014)? Or do they have an external origin (e.g. Ceverino et al. 2015)? In the latter case, are they small companion galaxies that merged with the host, or clumps of primordial gas that, flowing along the filaments of the cosmic web, have been accreted before starting to form stars?

If clumps (or part of them) are formed in-situ in their host galaxy, some newly born ones should be observed: capturing the early formation of clumps is one of the main challenges that future instruments could achieve. So far, most of the studies have selected clumpy galaxies in observed optical and/or IR broadband imaging, and stellar population modelling has revealed a wide range of ages for those clumps (Elmegreen et al. 2009; Guo et al. 2012; Elmegreen et al. 2013; Guo et al. 2015), with average age  $\sim$ 100 Myr. However, the continuum alone cannot robustly pinpoint ages  $<$ 30 Myr (Wuyts et al. 2012) and therefore spectroscopy, sensitive to the gas ionized by very young stars, is needed. An instrument enabling us to reach  $V \geq 27$  AB mag in the continuum and to simultaneously analyze spatially-resolved emission lines (e.g. with an IFU) will be critical to pinpoint newly born clumps with high equivalent width (EW, namely the ratio between the flux of an emission line and its underlying continuum) and to estimate their age with the aid of stellar population modelling.

The assembling of statistical samples of young clumps will also, indirectly, shed light on the following questions: are indeed high-redshift disks gas-rich and gravitationally unstable? What is the contribution of cold flows to the gas replenishment of galaxies? Are they smooth streams of gas or are they clumpy and therefore trackable through the observation of their densest peaks? What is the importance of minor mergers for high-redshift star formation?

### 3.3.1.3 What is clumps role in galaxy bulge formation?

Analogously, a hot debate is going on regarding clumps fate. The open question is whether giant clumps are long-lived phenomena (lifetime  $\sim$ 500 Myr) and eventually migrate, due to gravitational torques and dynamical friction, toward the center of the galaxy. At the center of the host potential well they might coalesce forming the bulge and feeding with gas the central supermassive black hole (e.g. Gabor & Bournaud 2013, Bournaud et al. 2014; Mandelker et al. 2017). If this scenario is observationally confirmed, clumps might have a crucial role in the morphological and structural evolution of galaxies, and their inward migration could potentially be an efficient mechanism to form bulges, alternative to galaxy major mergers. On the contrary, some simulations suggest a conflicting scenario where clumps are disrupted by stellar feedback in short timescales (e.g. Genel et al. 2012; Hopkins et al. 2014; Oklopcic et al. 2016). In this case they would just be short-lived, transient phenomena (lifetime  $\sim$ 50 Myr) with little or no impact on galaxy evolution. The main difficulty of addressing this issue with numerical simulations arises from the fact that stellar feedback is still poorly understood and can only be modelled through highly uncertain sub-grid models. Observations are therefore needed to bypass the *impasse*, securely determine

clumps' lifetime, and put constraints on the strength of stellar winds. A possibility is to gather statistical samples of clumps with accurate enough age estimate (e.g. determined through spatially-resolved spectral energy distribution fitting, Guo et al. 2012, Wuyts et al. 2013) and look for gradients as a function of their distance from the galaxy nucleus. In fact, if clumps survive stellar feedback and migrate inward as time passes, we expect to find, on average, older clumps at smaller radii. This has been clearly shown by simulations (e.g. Mandelker et al. 2014), but observationally statistical samples of clumps are still limited and their age estimates are quite uncertain. A new instrument allowing us to observe clumpy galaxies using multiple optical filters will be crucial to get better constraints on clump ages. Furthermore, its large field of view would be optimal to improve the current statistics: based on rest-frame UV *HST* observations in the Hubble Deep Field ( $5\sigma$  sensitivity  $\sim 27$  AB mag assuming  $0.2''$  apertures) we have estimated that in an area of  $\sim 30'' - 40''$  we expect to find  $\sim 5 - 7$  clumpy galaxies.

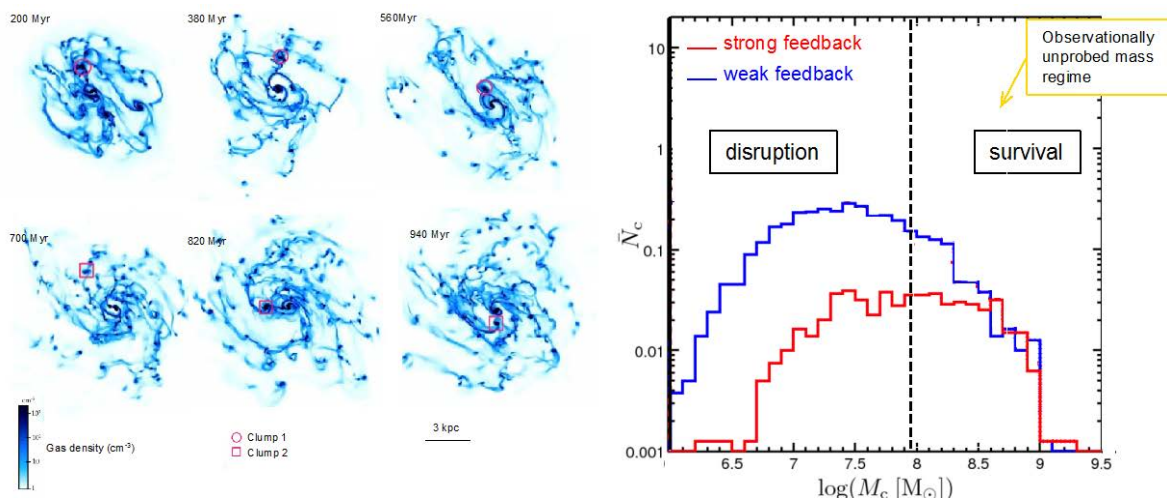


**Figure 3: Simulations of clumpy galaxies.** Left panels: snapshots taken at subsequent times showing the gas density distribution for a typical clumpy galaxy from high-resolution hydrodynamical simulations. Two typical clumps were selected and marked with symbols on the maps to show their evolution. Once they merge with the central disk or bulge or with another giant clump they are unmarked (Bournaud et al. 2014). Right panel: clumps mass function from cosmological simulations, assuming two different feedback recipes (including or not radiation pressure). In these simulations, independently of the assumed feedback, clumps with stellar masses  $\leq 10^8 M_\odot$  are rapidly disrupted, whereas the most massive ones have lifetimes of  $\sim 500$  Myr. The mass regime  $\sim 10^8 - 10^{8.7} M_\odot$  has not been observationally constrained so far (Mandelker et al. 2015).

If not only photometry, but also IFU spectroscopy will be available, one alternative and very promising way of proceeding is to find young clumps and estimate the clumps formation rate (CFR). Observationally, it can be determined with a sample of clumps caught at birth, when they are expected to rapidly collapse and form stars with a violent burst-like behaviour (Bournaud et al. 2014; Zanella et al. 2015). Given the timing constraint from the starburst event, and the observed number of newly formed clumps per galaxy, the CFR can be estimated. Finally, by comparing it with the average number of older descendants observable



per galaxy yields the average clumps' lifetime. From current simulations we expect an average of 5 clumps per galaxy with  $10^8 \leq M_{\text{star}}/M_{\text{sun}} \leq 10^{9.5}$  and therefore a CFR  $\geq 0.1 \text{ Myr}^{-1}$  in the short-lived case (lifetime  $\leq 50 \text{ Myr}$ ) and  $\sim 0.01 \text{ Myr}^{-1}$  in the long-lived (lifetime  $\sim 500 \text{ Myr}$ ) case. Considering that young clumps with extreme EW are visible for  $\sim 20 \text{ Myr}$ , we expect 1 – 2 young clumps per galaxy if they are short-lived and 1 – 2 every 10 galaxies if they are long-lived. An instrument with a large field of view will therefore be needed to gather statistically significant samples of young clumps and get a CFR and lifetime estimate accurate enough to discern among the different theoretical models. As a consequence, it will also indirectly constrain the strength of stellar feedback in high-redshift environments.

Furthermore, current high-redshift observations can only probe the most massive clumps ( $M_{\text{star}} \geq 10^9 M_{\text{sun}}$ ). Observational studies of intermediate-mass clumps ( $M_{\text{star}} \sim 10^8 - 10^9 M_{\text{sun}}$ ) are still lacking, although they are expected to be the most numerous and potentially most critical for bulge growth (Bournaud et al. 2015). Based on numerical simulation results, at lower masses the number of clumps is expected to increase substantially ( $N_{\text{clumps}} \sim M_{\text{clumps}}^2$ ): the clumps that contribute most to bulge formation have masses  $\sim 10^{8.5} M_{\text{sun}}$ , since more massive ones are relatively rare and those with smaller masses are disrupted by stellar feedback in short timescales (Figure 4, Mandelker et al. 2015). Current facilities are not suitable to investigate the parameter space spanning clumps' intermediate masses and low SFRs and therefore a new instrument providing exquisite spatial resolution and flux sensitivity will be crucial to push observations towards this unexplored regime.

### 3.3.1.4 How does the clumps' UV spectrum look like?

A new optical, diffraction-limited instrument with available spectroscopy would allow us to study the rest-frame UV spectrum of clumps, an achievement never reached so far. Current AO assisted spectroscopy in fact only allows us to probe clumps spectra down to rest-frame optical wavelengths (see Section 3) and therefore the characteristics of clumps' UV emission lines are still unknown. In particular, the brightness of the C III]λ1909, He IIλ1640, and Mg IIλ2798 lines can be used, under the guidance of photoionization modelling predictions, to constrain the clumps' initial mass function (IMF). Emission lines brighter than  $5 - 9 \times 10^{-18} \text{ erg s}^{-1} \text{ cm}^{-2}$  in fact would signal a hard ionizing radiation, likely due to numerous O-type stars. Assuming a standard IMF, these fluxes would imply an unrealistic stellar mass, then pointing toward a more exotic IMF (e.g. top-heavy IMF, Baugh et al. 2005). This could be plausible for star-forming clumps, especially considering their enhanced star formation efficiency and starburst-like behaviour.

Furthermore, with enough spectral resolution (needed resolving power R  $\sim 4000$ ) it will be possible to analyze the C III]λ1909, He IIλ1640, and Mg IIλ2798 emission line profiles to check for the presence of broad components that could constrain the strength of stellar winds. This would be very useful to understand the clumps' nature.

Another possibility to constrain supernovae outflows is to analyze the Lyα line, which is expected to be the brightest emission in the wavelength range covered by the V band. Its peak position together with the asymmetry of its profile, with the aid of accurate radiation transfer modelling, can give important insights into the presence of outflowing (or sometimes infalling) material, the neutral hydrogen column density, and the geometry of the region where the line originates from (Verhamme et al. 2006). Additionally, the Lyα emission together with the Lyman continuum can be used to constrain the Lyman continuum escape



fraction in clumps (Verhamme et al. 2015, Verhamme et al. 2017). Given their high EW and starburst-like nature, clumps could behave as small analogs of the recently discovered “green peas” (Cardamone et al. 2009; Izotov et al. 2011; Jaskot & Oey 2013), compact galaxies with green colors due to intense [OIII] emission that seem to be strong Lyman continuum leakers (beyond being strong Ly $\alpha$  emitters). This completely unexplored domain could reserve major surprises about clumps’ physical properties and their influence on the host galaxy evolution and characteristics.

Finally, UV emission lines could allow us to estimate temperature and density of the gas ionized by star formation, and to assess the observationally unexplored gas conditions in high-redshift clumps: is the gas multiphase? Is molecular gas continuously forming stars, while the ionized gas is only a small fraction of the total? Or is the gas fully ionized when a new clump is formed and only later it cools down and forms new stars?

### 3.3.2 Why is a new instrument needed

Probably the main reason why *HST* revolutionized the field of galaxies formation and evolution has been the simultaneous improvement, for both photometric and spectroscopic observations, in spatial resolution and flux sensitivity, combined with its relatively large field of view. It allowed to study high-redshift galaxies with unprecedented detail and to go beyond the crude analysis of their global, average properties. A similar resolution from the ground can now be achieved with the *VLT/SINFONI* integral field spectrograph at NIR wavelengths. At  $z \sim 2$  it probes the well known hydrogen lines ( $H\alpha$  and  $H\beta$ ) together with the typically bright oxygen lines ([OIII] and [OII]). Its main limitation however, is the small field of view (at most  $8'' \times 8''$ ) that basically only allows to observe one high-redshift galaxy at the time. Gathering large statistical samples of targets is therefore unworkable due to the too long needed integration time. Another limitation of SINFONI is the need of a bright star to be used for the AO correction close enough to the target galaxy, a constraint that is often difficult to fulfil in extragalactic fields. A larger AO corrected field of view will be offered soon by the Wide Field Mode of *VLT/MUSE*, but its spatial resolution will be  $\sim 0.4''$  (at  $z \sim 2$  it corresponds to  $\sim 3.5$  kpc), which is too coarse to study clumps and start to resolve them. Much better resolution ( $\sim 0.05''$ ) will be soon available with its Narrow Field Mode, but the small field of view ( $7.5'' \times 7.5''$ ) only allows to observe one target at the time. Furthermore, the need for a bright (<15 mag) “TT star” within the field of view to have a full AO correction might be a major issue when observing high-redshift sources. Therefore, the possibility to have simultaneously imaging and spectroscopy in the rest-frame UV with stable diffraction-limited resolution across the entire field of view still remains a unique opportunity that could open unexpected frontiers. Finally, these data could complement the *JWST/MIRI* and *E-ELT/HARMONI* ones taken in the NIR: an optical instrument on an 8 m telescope as *VLT* can reach a similar resolution and depth obtained at NIR wavelengths by a ground-based 40 m telescope, therefore allowing us to carry on a multi-wavelength study of galaxies on kpc scales down to extremely faint fluxes.

### 3.3.3 Summary

Having an optical instrument on *VLT* with an even better spatial resolution than *HST* and a high flux sensitivity could allow in the near feature to study high-redshift galaxies with the same level of detail currently reached for local sources. Dissecting  $z \sim 2$  galaxies down to kpc scales will be a big step toward the comprehension of the mechanisms driving bulge formation



and feeding the central supermassive black hole. It will be possible to understand how giant star-forming clumps are formed and therefore which are the main channels through which galaxies are replenished with new gas. The gas conditions in the clumps themselves will be investigated through the analysis of spatially resolved emission line maps and the comparison with photometric data. Finally, by comparing high- and low-redshift observations taken with similar spatial resolution it will be possible to investigate the evolution of clumps properties across cosmic time. A large field of view will be crucial to gather statistical samples of galaxies and obtain robust and accurate results. Should the optical observations match the *E-ELT* spatial resolution and depth in both NIR spectroscopy and imaging, we could carry on kpc-scale multi-wavelength studies of galaxies interior, reaching a more comprehensive understanding of their evolution, and exposing us to great surprises and more discoveries.

## References

- Abraham, R. G., van den Bergh, S., Glazebrook, K., et al., 1996, ApJS, 107, 1
- Baugh, C. M., Lacey, C. G., Frenk, C. S., et al., 2005, MNRAS, 356, 1191
- Bournaud, F., Daddi, E., Weiβ, A., et al., 2015, A&A, 575, A56
- Bournaud, F., Dekel, A., Teyssier, R., et al., 2011, ApJL, 741, L33
- Bournaud, F., Perret, V., Renaud, F., et al., 2014, ApJ, 780, 57
- Cardamone, C., Schawinski, K., Sarzi, M., et al., 2009, MNRAS, 399, 1191
- Ceverino, D., Dekel, A., Tweed, D., & Primack, J., 2015, MNRAS, 447, 3291
- Conselice, C. J., 2014, ARA&A, 52, 291
- Cowie, L. L., Songaila, A., Hu, E. M., & Cohen, J. G., 1996, AJ, 112, 839
- Elmegreen, B. G., & Elmegreen, D. M., 2005, ApJ, 627, 632
- Elmegreen, B. G., Elmegreen, D. M., Fernandez, M. X., & Lemonias, J. J., 2009, ApJ, 692, 12
- Elmegreen, B. G., Elmegreen, D. M., Sánchez Almeida, J., et al., 2013, ApJ, 774, 86
- Fisher, D. B., Glazebrook, K., Damjanov, I., et al., 2017, MNRAS, 464, 491
- Förster Schreiber, N. M., Shapley, A. E., Genzel, R., et al., 2011, ApJ, 739, 45
- Gabor, J. M., & Bournaud, F., 2013, MNRAS, 434, 606
- Genel, S., Naab, T., Genzel, R., et al., 2012, ApJ, 745, 11
- Genzel, R., Burkert, A., Bouché, N., et al., 2008, ApJ, 687, 59 Genzel, R., Newman, S., Jones, T., et al., 2011, ApJ, 733, 101
- Guo, Y., Ferguson, H. C., Bell, E. F., et al., 2015, ApJ, 800, 39
- Guo, Y., Giavalisco, M., Ferguson, H. C., Cassata, P., & Koekemoer, A. M., 2012, ApJ, 757, 120
- Hopkins, P. F., Kereš, D., Oñorbe, J., et al., 2014, MNRAS, 445, 581
- Izotov, Y. I., Guseva, N. G., & Thuan, T. X., 2011, ApJ, 728, 161



- Jaskot, A. E., & Oey, M. S., 2013, ApJ, 766, 91
- Jones, T. A., Swinbank, A. M., Ellis, R. S., Richard, J., & Stark, D. P., 2010, MNRAS, 404, 1247
- Madau, P., & Dickinson, M., 2014, ARA&A, 52, 415
- Mandelker, N., Dekel, A., Ceverino, D., et al., 2014, MNRAS, 443, 3675
- Mandelker, N., Dekel, A., Ceverino, D., et al., 2015, arXiv:1512.08791, MNRAS, submitted  
—, 2017, MNRAS, 464, 635
- Oklopcic, A., Hopkins, P. F., Feldmann, R., et al., 2016, arXiv:1603.03778, MNRAS, submitted
- Swinbank, A. M., Smail, I., Chapman, S. C., et al., 2010, MNRAS, 405, 234
- van den Bergh, S., Abraham, R. G., Ellis, R. S., et al., 1996, AJ, 112, 359
- Verhamme, A., Orlitová, I., Schaerer, D., & Hayes, M., 2015, A&A, 578, A7
- Verhamme, A., Orlitová, I., Schaerer, D., et al., 2017, A&A, 597, A13
- Verhamme, A., Schaerer, D., & Maselli, A., 2006, A&A, 460, 397
- Wuyts, S., Förster Schreiber, N. M., Genzel, R., et al., 2012, ApJ, 753, 114
- Wuyts, S., Förster Schreiber, N. M., Nelson, E. J., et al., 2013, ApJ, 779, 135
- Zanella, A., Daddi, E., Le Floc'h, E., et al., 2015, Nature, 521, 54



### 3.4 The hunt for intermediate-mass black holes in globular clusters

By Andrea Bellini, STScI, USA

The existence of black holes (BHs) in the stellar-mass ( $\sim 5 - 20 \text{ M}_{\odot}$ ) and supermassive ( $\sim 10^6 - 10^{10} \text{ M}_{\odot}$ ) ranges has been established beyond reasonable doubt, from observations in many wavelengths. By contrast, the possible existence of intermediate-mass BHs (IMBHs;  $\sim 10^2 - 10^4 \text{ M}_{\odot}$ ) in the Universe remains a debated issue. Identification of IMBH signatures has been argued, e.g., from observations of globular cluster (GC) centers and ultraluminous X-ray sources (see review by van der Marel 2004, in Coevolution of Black Holes and Galaxies). However, the majority of the evidence remains circumstantial and open to alternative interpretations.

If IMBHs exist, they would be of great astrophysical interest. They may hold keys to unveiling the assembly of supermassive BHs at high redshifts, and may tell us about the first (Population III) stars to form in the Universe (e.g., Volonteri et al. 2003, ApJ, 582, 559). They could also be gravitational-wave sources with unique information content in both ground-based and space-based detectors (e.g., see Miller & Hamilton 2002, MNRAS 330, 232; Abbott et al. 2016, Phys. Rev. Lett. 116, 061102).

Globular clusters are considered promising candidates to host an IMBH in their center. When they were young, their dynamical state may have been favorable for runaway mergers of massive stars (Portegies Zwart et al. 2004, Nature 428, 724). Possible mass ratios resulting from this process are  $M_{\text{BH}}/M_{\text{GC}} \approx 0.1\%$ , consistent with extrapolation of the  $M_{\text{BH}} - \sigma$  relation for supermassive BHs to GC masses (e.g., Tremaine et al. 2002, ApJ 574, 740). However, direct detection of IMBHs in GCs is extremely challenging.

Globular clusters are gas poor, hence X-ray and radio emission is expected to be faint. Deep searches for such emission in a dozen clusters have provided mostly IMBH upper limits, clustered around the predictions from the  $M_{\text{BH}} - \sigma$  relation (Maccarone & Servillat 2008, MNRAS, 2008, 389, 379). The sole exception is G1, the most massive GC of M31, for which radio and X-ray detections are consistent with a  $M_{\text{BH}} \sim 2 \times 10^4 \text{ M}_{\odot}$  (Ulvestad et al. 2007, ApJ, 661, L151). Recent observations (Wrobel et al. 2012, AAS 219 247.01), though, indicate that the radio signature may be transient, suggesting a non-IMBH origin.

An IMBH should affect the density profile of a GC (Bahcall & Wolf 1978, ApJ 209, 214). The associated surface-brightness profile in the central region of a GC should have a large core with a central shallow cusp (Baumgardt et al. 2005, ApJ 620, 238; Trenti et al. 2007, MNRAS 374, 857). While this signature is observed in some GCs (Noyola & Gebhardt 2006, AJ 132, 447), it is not uniquely associated with the presence of an IMBH (Trenti, Vesperini, & Pasquato 2010, ApJ, 708, 1598).

Kinematic measures can in principle directly probe the gravitational influence of an IMBH in GCs. However, this is demanding because the kinematic signature is limited to the IMBH sphere of influence, which typically of the order of  $\sim 1''$ . Crowding in this region makes measurement of line-of-sight (LoS) velocities of individual stars challenging, even with the Hubble Space Telescope (HST, van der Marel et al. 2002, AJ 124, 3255). The LoS velocity dispersion can alternatively be measured from integral-field units (IFUs), but in this case the result is affected by shot noise from the brightest giant stars. For these reasons, all reported IMBH detections from LoS dispersion profiles have been disputed in the literature. This includes M15 (Gerssen et al. 2002, AJ, 124, 3270; Gerssen et al. 2003, AJ 125, 376, versus



Baumgardt et al. 2003, ApJ, 582, L21), G1 (Gebhardt et al. 2002, ApJ 578, L41; Gebhardt et al. 2005, ApJ, 634, 1093, versus Baumgardt et al. 2003, ApJ, 589, L25), and omega Centauri (Noyola et al. 2008, ApJ, 676, 1008, versus. van der Marel & Anderson 2010, ApJ, 710, 1063).

A significant improvement in data quality is possible with PM measurements. Proper motions are small and difficult to measure, and require sophisticated, state-of-the-art reductions tools (see, e.g., Bellini et al. 2014, ApJ, 797, 115). Nevertheless, PMs offer many advantages over LoS velocity studies: (1) No spectroscopy is required, so fainter stars can be studied, which yields better statistics on the kinematical quantities of interest; (2) Stars are measured individually, by contrast to integrated-light measurements, so a disproportionate contribution from bright giants is avoided; (3) Two components of velocity are measured (tangential and radial), instead of just one, which doubles the statistics. More importantly, PMs directly constrain the velocity-dispersion anisotropy of a GC system, addressing the mass-anisotropy degeneracy (Binney & Mamon 1982, MNRAS, 200, 361). The centermost regions of GCs are often too crowded even for the exquisite spatial resolution of HST (see, e.g., Bellini et al. 2014, ApJ, 797, 115). The best HST instrument with the potential to discover IMBHs in GCs via PMs was the high-resolution channel (HRC) of the advanced camera for surveys (ACS). Unfortunately, both sides of the electronics of ACS failed in 2007, and the HRC was not brought back to life during the HST Servicing Mission 4 in 2009. The HRC had a pixel scale of about 26 mas/pixel and a field-of-view (FoV) of about 29x26 arcsec<sup>2</sup>.

The diffraction-limited optical imager mounted on the VLT would provide the scientific community with the best-possible tool to-date to hunt for IMBHs in GCs. In fact, its resolving power (17 mas and 10-20% Strehl ration in V-band) would be comparable to that of the HST's ACS/HRC, and a factor ~3 better than what HST can currently do. Two key calibration factors need to be addressed in order to achieve state-of-the-art PM measurements: high-precision point-spread function (PSF) models and high-precision geometric-distortion (GD) solutions. The expected high variability of the PSF in AO detectors, both spatially across the FoV and from one image to the next, will not be an issue for this particular science case. The cores of GCs contain thousands of stars that can be observed in each individual exposure within a FoV of 30x30 arcsec<sup>2</sup> and a diffraction-limited camera. These stars can be used to obtain high-precision, spatially-varying empirical PSF models for each exposure, as it is now routinely done even for HST (e.g., Bellini et al. 2013, ApJ Letters, 769, 32; Bellini et al. 2017, ApJ in press, arXiv: 1704.07425). The geometric distortion is expected to only have a marginal impact in narrow-field AO detectors. Yet, an adequate characterization of the GD distortion is required for high-precision PM measurements. Such characterization can only be obtained with high-precision PSF models (Anderson & King 2002, PASP, 115, 113). Moreover, having at disposal thousands of stars and appropriate PSF models will allow us to minimize even the most subtle observation-dependent variations of the GD. All in all, no other instrument would be able to pave the path to IMBH discoveries as the optical AO imager at the VLT.



## 3.5 Spatially Resolved Absorption Lines

By Celine Peroux, University of Marseille, France, currently guest at ESO

**Abstract:** Baryons from the cosmic web accrete onto galaxies, cool into a dense neutral then a molecular phase which fuels star formation, expelling material from these galaxies in powerful outflows which transform the surrounding circumgalactic medium (CGM). Today, the lack of observational constraints limits our understanding of these phases of the gas and its metallicity. A powerful tool to study the low-density gas is offered by absorption lines in quasar spectra, although the information retrieved is limited to one dimension along the line-of-sight. Extended background galaxies however will provide spatial distribution, clumpiness, cloud size and hence mass of these absorption lines as well as crucial measurements of metal-missing in the intergalactic medium on small scales (<1kpc). Such observations require a new diffraction limited VLT optical instrument equipped with (3d) spectroscopy capabilities and an extended blue coverage.

### 3.5.1 Background

We now know the basic constituents of the present Universe: 73% dark energy, 23% dark matter, 4% in baryons of which only 0.4% is in stars. Therefore, only a minority of the normal matter can be probed by the observations of starlight from galaxies, *the remaining 90% of the baryons are traced by the intergalactic gas*. In addition, galaxy formation is known to be fed by inflows of gas from the intergalactic medium-IGM (e.g. Dekel et al. 2009). Once formed, galaxies interact with the IGM by polluting it with ionising photons and heavy elements formed in stars and supernovae, and by driving galactic winds into the IGM (Pettini et al. 2003; Shull, Danforth & Tilton 2014). The feedback processes of photo-ionisation (and photo-heating), chemical enrichment, and shock-heating of the IGM by the first stars and galaxies profoundly affects the formation of subsequent generations of galaxies. Much attention has been focused on the circumgalactic medium (CGM), a loosely defined term which describes the gas immediately surrounding galaxies (Ford et al. 2014).

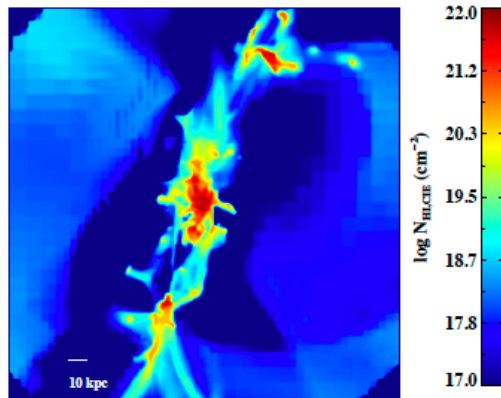


**Figure 1:** Hydro cosmological simulations of the neutral hydrogen column density map at  $z=2.3$ . The NHI is from collisional ionisation processes as most of the gas that resides in the streams is ionised by electron collisions (and the UVB). This figure illustrates the complex morphological structure expected from quasar absorbers, even at the higher end of the column density distribution (from Fumagalli et al. 2011).

It is of utmost importance to study gas flows into and out of galaxies simultaneously as their mutual interactions affect each other (as illustrated in Figure 1 from Fumagalli et al. 2011; see also Stewart et al. 2011; Stinson et al. 2012; Rudie et al. 2012). Accretion is required to explain some of the basic observed properties of galaxies including the gas-phase metallicity (e.g. Erb et al. 2006). Moreover, galaxies are believed to interact with the IGM by filling it with ionising photons and by injecting heavy elements formed in stars and supernovae through these supersonic galactic winds. The metals carried by the outflow will either rain back on to the galaxy or get mixed into the IGM, although this mixing could remain incomplete (e.g. Dedikov & Shchekinov 2004). Indeed, observations of the IGM indicate significant quantities of metals at all redshifts (Pettini et al. 2003; Ryan-Weber et al. 2009; D'Odorico et al. 2013; Shull, Danforth & Tilton 2014). The presence of these metals is interpreted as a signature of strong galactic outflows in various models (Aguirre et al. 2001; Oppenheimer & Dave 2006). Hydrodynamics simulations provide predictions of the physical properties of these gas flows, but many issues remain unsolved (Keres et al. 2005; Brook et al. 2011). For example, it is still debated whether the cold gas streams seen in hydrodynamics simulations are a real physical feature or are related to a numerical/resolution problem (Sijacki et al. 2012). Another question is if the heavy elements that end up in the IGM were initially concentrated in gas clouds with very high metallicities, then what about the intermediate phase? Where are the high-metallicity, intergalactic gas clouds? Observing this phase is very important because it will give us valuable information regarding the physics of galactic winds, a key ingredient of theories of galaxy formation, and the enrichment of the IGM.

A powerful tool to study the low-density gas is offered by absorption lines in quasar spectra. In these quasar absorbers, the minimum gas density that can be detected is set by the brightness of the background source and thus the detection efficiency is independent of redshift. High-quality quasar absorption spectra have produced a wealth of information regarding the distribution of heavy elements in the high-redshift IGM. However, the brightest



background sources (quasars and gamma-ray bursts) are point-source so that the observer is limited to the information gained along the line-of-sight. These measurements implicitly smooth over the scales associated with typical HI Ly $\alpha$  absorbers,  $R=100$  kpc depending on the density (see Schaye et al. 2003; Schaye & Aguirre 2005 for discussions). **On smaller scales the distribution of metals is essentially unknown.** The next step is therefore to map the under-dense intergalactic medium and in particular the area around galaxies where these interact with their medium.

### 3.5.2 Spatially Resolved Absorption Lines:

Quasar absorbers observed in sightlines to bright quasar and gamma ray bursts yield a wealth of information, such as their chemical composition, ionisation states and gas kinematics, but the background sources only probe areas  $<0.01$  pc $^2$  (1 pc = 3.26 light years). Recently, Bergeron & Boisse (2017) have studied absorption line profiles fortuitously lying on more extended quasar emission line regions ( $\sim 0.3\text{--}1$  pc) and compare them with absorption lines again the same quasar continuum to estimate the covering factor of the absorbing gas. By studying quasar absorbers in galaxy sightlines, thereby providing even more extended background sources (on kpc scale), one can start to map the distribution and sizes of the absorber. Figure 2 illustrates how this set-up allow to probe the spatial distribution, clumpiness and cloud sizes, which in turns allow one to put direct constraints on the gas mass.

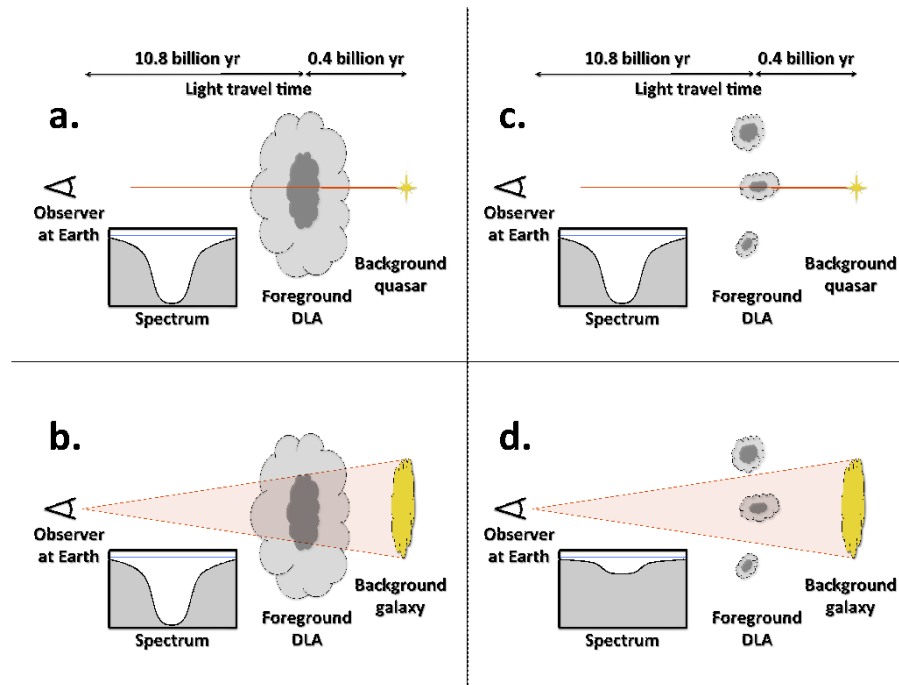


**Figure 2: Absorption lines observed with resolved background sources.** In cases where the background source probes the high column density region (dark grey) of the quasar absorbers (a, b, & c), the spectrum exhibits strong Ly $\alpha$  absorption with damping wings. When a fraction of the background source flux travels unimpeded past the quasar absorbers, a net shallower absorption and damping wing profile results. Quasars cannot distinguish between scenarios (a) and (c) and only indicate that the quasar absorbers are as large or larger than their size ("0.01 pc<sup>2</sup>). However, background galaxies assess DLA sizes out to their full luminosity extent (~1–100 kpc<sup>2</sup>) from the absorption feature depth and profile (from Cooke & O'Meara, private communication).

In addition, Schaye et al. (2007) report that direct observations of the sizes of individual metal-line clouds, including CIV, typically find very small sizes. These observations do not attempt to select high-metallicity gas, except for the unavoidable condition that the metal line be detectable. This suggests that intergalactic metals generally reside in small patches of gas. Although the clouds expand until they become part of the IGM, the metals remain poorly mixed on scales greater than 1 kpc for very low overdensities and on even smaller scales for higher densities. The metallicity we typically infer from absorption studies is then not determined by the abundances of heavy elements on the size of the metal concentrations, but by the metallicity smoothed over the size of the HI absorber, which is well known to be much greater. *This scenario has some profound implications.* When smoothed on small scales (kpc), most of the IGM (which contains most of the baryons in the universe) may be of primordial composition. A very small amount of intergalactic gas is, however, metal rich. Such pockets of metal-rich material will cool more efficiently, which may change the physics of galaxy formation. The number of metal line components per HI



absorber depends on the number of metal concentrations along the line of sight. The absence of associated absorption by heavy elements, even in a spectrum with an infinite signal-to-noise ratio, does not necessarily imply that the HI absorber is metal free. *Therefore, the only way to test this poor-metal mixing scenario is to spatially resolved absorption lines on scales below 1kpc.*

### 3.5.3 Technical Requirements (Desirables):

The proposed experiment will only be possible thanks to the next leap forward offered by a diffraction limited VLT optical instrument. Below, we detail the four major technical requirements:

- 1) *3D Spectroscopy*: characterising the physical properties of the intervening gas relies on spectroscopy of the background source. An Integral Field Spectrograph (IFU) will allow to resolve spatially the properties of the absorbing gas trace by Ly $\alpha$  and metal lines. The size of the IFU should be several arcseconds to fully cover the extend of the redshifted background source. Alternatively, a long slit could be used sliding along the object but would reduce considerably the total acquisition time and complicate the data reduction.
- 2) *Blue wavelength coverage*: an extended blue coverage down to  $\lambda = 3500$  Ang will allow us to cover closer background objects which in turns will be significantly brighter as the surface brightness of the background source scales as  $(1+z)^{-4}$ . In addition, it will provide an extended coverage in Ly $\alpha$  (1216 Ang) to lower redshifts thus increasing the redshift path along the line of sight to  $z>1.8$  and in a domain where the Ly $\alpha$  forest is thinner.
- 3) *Spatial resolution*: the unprecedented spatial resolution at these wavelengths is key to reach the smallest possible scales in absorption. Typically, at  $z=2.4$ , the 7-8 mas pixel scale will probe the physical conditions of the gas on 60pc scales.
- 4) *Sensitivity*: the extended background sources are bound to have low surface brightnesses ( $V\sim 24$ ) hence high sensitivity is key to undertake this project.

### 3.5.4 Competitors:

The MUSE Narrow Field Mode (NFM) with a pixel scale of 25 mas over a field-of-view 7.5"x7.5" might at first appear suitable for this science case. Indeed, the blue coverage ( $\lambda > 4900$  Ang; corresponding to  $z_{Ly\alpha} > 3.0$ ) and sensitivity  $RAB<22.3$  in 1 hr might appear suitable. However, this mode requires a tip-tilt "star" with magnitude of <15 mag in J-H in the field which precludes observations of cosmological fields as the ones required here.

On the other hand, the HARMONI IFU instrument planned for the ELT will offer several modes. The largest pixel scale of 60x30 mas leads to a field-of-view of 6.42"x9.12", while the smallest pixel scale of 4 mas corresponds to 0.61"x0.86". The expected sensitivity is  $RAB<22.2$  with a spectral resolution  $R=3000, 7000$  or  $20\,000$ . The instrument's wavelength

coverage is 4700-24500 Ang (corresponding to  $z_{\text{Ly}\alpha} > 2.9$ ) but the AO correction is from 8000 Ang redwards. The proposed diffraction limited VLT optical instrument therefore complements the ELT/HARMONI capabilities at redder wavelengths.

Finally, LUVOIR, one of the four concept-missions for the NASA decadal survey would be very suitable for this science case at low-redshift, although an IFU mode is unlikely. The Phase 0 study for LUVOIR started in October 2016 and the final reports to the NASA decadal survey are planned for March 2019 for a launch around 2035. The early stage of the project and likely timeline of this ambitious mission are therefore not in competition with the current proposal.

### 3.5.5 Potential Targets:

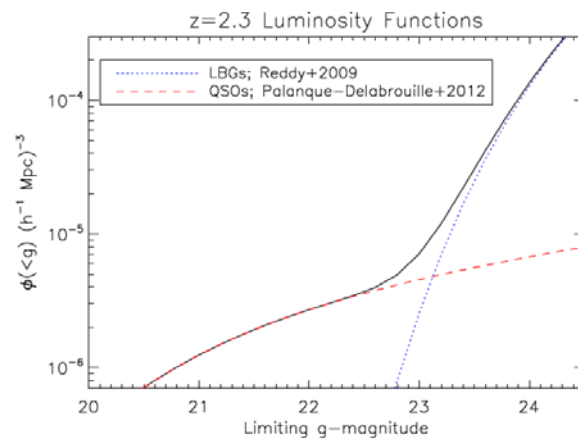


**Figure 3: Luminosity functions as a function of limiting g magnitude. The red dashed curve shows the QSO luminosity function from Palanque-Delabrouille et al. (2013), while the dotted blue curve is the LBG luminosity function from Reddy et al. (2008). The solid curve shows the sum of both luminosity functions. At fainter magnitudes, unresolved galaxies outnumber quasars (from Lee et al. 2014).**

Figure 3 demonstrates how at fainter magnitudes, unresolved galaxies outnumber quasars. These extended background galaxies will be ideal targets to observe spatially resolved absorption lines. In an early work, Cooke & O'Meara (2015) have reported the discovery of a high-column-density ( $\log N(\text{H I}) = 21.1 \pm 0.4 \text{ cm}^{-2}$ ) DLA at  $z \sim 2.8$  covering 90%–100% of the luminous extent of a  $z \sim 2.8$  line-of-sight background galaxy ((V~24)). Estimates of the size of the background galaxy range from a minimum of a few  $\text{kpc}^2$  to  $\sim 100 \text{ kpc}^2$  and demonstrate that high-column-density neutral gas can span continuous areas 108–1010 times larger than previously explored in quasar or gamma-ray-burst sightlines. The authors advocate that the most physically compact morphology to produce such star forming galaxy would be that of a highly dense  $\sim 1 \text{ kpc}$  super-star-forming clump. Such a compact background galaxy would probe continuous areas of the quasar absorbers  $> 100,000,000$  larger than that probed by quasars and gamma-ray-burst sightlines. The authors stress that this quasar absorber is the first from a sample in a pilot survey that searches Lyman break and Lyman continuum galaxies at high redshift.

Similarly, in recent observations with the MUSE IFU, we have serendipitously discovered a



$z \sim 1.06$  MgII/Fell absorber in the spectrum of a  $z \sim 1.14$  background galaxy extended over 1 arcsecond. The MUSE pixel scale (0.2'') at the redshift of the absorber translates into 5x5 resolution elements of  $\sim 1.6$  kpc size. In addition, two emitting galaxies are observed in OII at the redshift of the absorber with angular separations of the order  $\sim 30$ kpc. The treasure trove of MUSE cubes now available in the ESO archives are bound to provide numerous additional metal absorbers at low redshifts.

### 3.5.6 Conclusions

A diffraction limited VLT optical instrument equipped with (3d) spectroscopy capabilities and an extended blue coverage will allow us for the first time to observe spatially resolved absorption lines again extended background galaxies. These observations will probe the spatial distribution, clumpiness and cloud sizes, which in turns allow one to put direct constraints on the gas mass of the absorbers. It will also be the ultimate test to the poor-metal mixing scenario by spatially resolving absorption lines on scales below 1kpc.

### References:

- Aguirre, Hernquist, Schaye, Weinberg, Katz & Gardner, 2001, ApJ, 560, 599  
Bergeron & Boisse, 2017, arXiv:1705.05131  
Brook et al. 2011, MNRAS, 415, 1051  
Cooke & O'Meara, ApJL, 2015, 812, 27  
Dedikov, Shchekinov & Yu, 2004ARep...48....9  
Dekel, et al. 2009Natur.457..451  
D'Odorico et al. 2013, MNRAS, 435, 1198  
Erb et al. 2006, ApJ, 644, 813  
Fumagalli, et al., 2011MNRAS.418.1796F  
Ford, et al. 2014MNRAS.444.1260  
Kereš, Katz, Weinberg, & Dav., 2005, MNRAS, 363, 2  
Lee et al. 2014, ApJ, 788, 16  
Oppenheimer & Dave, 2006, MNRAS, 373, 1265  
Palanque-Delabrouille, et al., 2013A&A...551A..29  
Pettini, Madau, Bolte, Prochaska, Ellison & Fan, 2003, ApJ, 594, 695  
Reddy, et al., 2008ApJS..175...48  
Rudie, Steidel, Trainor, Rakic, Bogosavljević, Pettini, Reddy, Shapley, Erb, Law, 2012, ApJ, 750, 67  
Ryan-Weber, Pettini, Madau & Zych, 2009, MNRAS, 395, 1476  
Schaye, et al. 2003ApJ...596..768  
Schaye & Aguirre, 2005IAUS..228..557  
Schaye, Carswell & Kim, 2007MNRAS.379.1169  
Shull, Danforth & Tilton, 2014, ApJ, 796, 49  
Sijacki et al. 2012, MNRAS, 424, 2999  
Stewart, Kaufmann, Bullock, Barton, Maller, Diemand, Wadsley 2011, ApJ, 738, 39  
Stinson et al. 2012, MNRAS, 425, 1270



## 3.6 Detecting low-mass dark matter haloes with gravitational lensing

By Simona Vegetti, Max Planck Institute for Astrophysics, Germany

### Abstract:

Dark matter is believed to make up to 85 percent of the total mass of the Universe, however most of its properties have yet to be constrained. All dark matter models predict that the dark matter distribution at small scales should be clumpy and that there should be a significant number of low-mass dark-matter haloes scattered around other more massive galaxies. At the same time the exact amount of these small haloes strongly depends on the assumed dark-matter model. Quantifying the clumpiness of the Universe at the smallest scales represents therefore a key probe on the nature of dark matter.

Gravitational lensing provides a unique channel to detect low-mass haloes beyond the local Universe inside massive ETGs and along their line-of-sight. However, there have been only three published detections to date. Moreover, these existing detections all probe the higher end of the dark-matter mass function, where there is a significant degeneracy between different feedback models and dark-matter models. To break this degeneracy it is necessary to decrease the detection threshold (i.e. lower the smallest detectable mass) below  $10^8$  solar masses. For a given signal-to-noise ratio, this can be achieved by increasing the angular resolution of the imaging, and or increasing the complexity of the data by targeting clumpy and compact star forming lensed galaxies.

A V-band diffraction limited optical camera with high angular resolution, would therefore provide a significant improvement on the (sub)structure sensitivity relatively to what is currently possible with the HST and it would be a key ingredient for probing the dark-matter mass function in a regime where prediction from different dark-matter models significantly differ.

### 3.6.1 Introduction

**Dark structures and the nature of dark matter:** One of the most robust results of the past 20 years of cosmological studies is the widespread presence of dark matter. Not only do we know that dark matter constitutes as much as 23 percent of the total matter content of the Universe (Planck Collaboration 2015), but we also have strong observational evidence that it must be some form of weakly interacting non-ordinary matter. However, as of today, little more is known about it. At present, mainly three independent and complementary approaches exist to help us reveal the nature of dark matter: (i) to directly produce dark matter particles using particle accelerators; (ii) indirectly and directly detect dark matter particles with specifically designed detectors; and (iii) measuring the level of clumpiness of the Universe at the smallest non-linear scales. The third approach is the main objective of this science case.

In all dark-matter models, structures in the Universe form in a hierarchical bottom-up fashion, where smaller structures (dark-matter haloes) form first and then merge together or accrete one another to form larger and larger structures. While most of the small

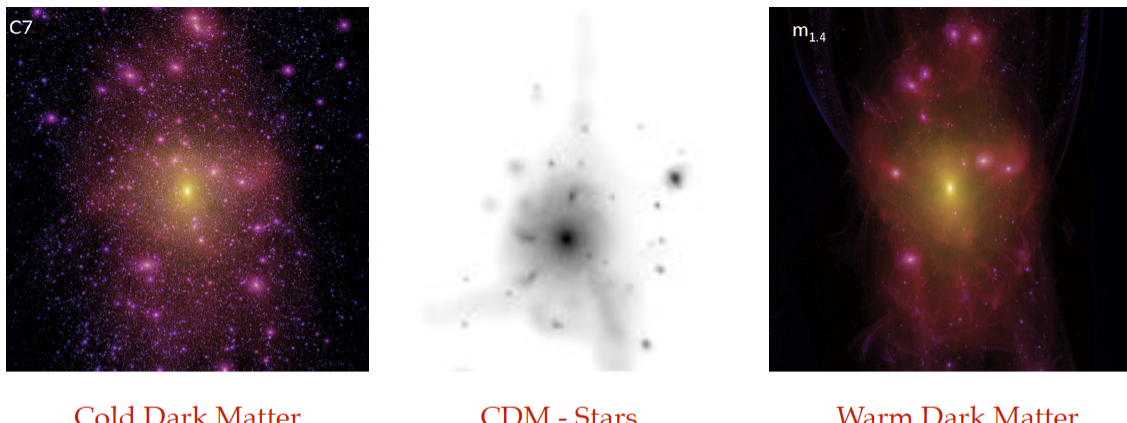


structures are destroyed and totally absorbed by the new larger ones, a significant number of them are able to survive till the present day in the form of substructure (subhaloes/satellites), gravitationally bound and orbiting within the halo of massive galaxies. An interesting aspect of these substructures is that their abundance strongly depends on the properties of dark matter, with galaxies in a Warm Dark Matter universe (WDM), or other alternative DM models having significantly fewer low-mass substructures than their counterparts in a Cold Dark Matter (CDM) model (e.g. Lovell et al. 2012, Figure 1). More specifically, the main difference between CDM and WDM is related to the free-streaming cut-off in the primordial power-spectrum of the density fluctuations; for keV-mass particles, the cutoff happens at the scale of dwarf galaxies, in the case of cold particles, it occurs on the scale of planets. Consequently, CDM models predict a steeply rising substructure mass function, while WDM models predict a cut-off mass below which the slope of the mass function flattens (Figure 2). Counting the number of galaxy satellites is therefore a clean and direct method to distinguish between different dark matter models.

**Detecting low-mass haloes with strong gravitational lensing:** As detecting low-mass structures is observationally challenging, most studies have been limited to the satellites of the Milky-Way and the Andromeda galaxies, but which may not necessarily be a fair representation of the Universe. One would like therefore to extend these studies to more distant galaxies, to improve their statistics, and study their evolution and their properties. In the future, even observations made with the next generation of large optical/infrared telescopes will only allow kinematical studies of dwarf satellites out to the Virgo cluster at about 20 Mpc away. Moreover, it is expected that the luminous satellites will form only a small fraction of the total number of galactic substructures and most of these low-mass substructures will be dark, and therefore, not directly observable with standard imaging techniques. In practice, there is an observational degeneracy between a CDM model, where most of the low-mass substructures are left dark, possibly due to the suppression of star formation in the low-mass haloes, and WDM models, where low-mass substructures are not formed in the first place (Figure 2).

Strong gravitational lensing is, at present, the only available method that allows to measure the amount of the small faint/dark satellites beyond the Local Universe, break this degeneracy and observationally probe the nature of dark matter. When the optical axis to a massive foreground object and a more distant source are sufficiently close, the light rays emitted by the source are strongly deflected as they pass through the foreground gravitational field, leading to the formation of multiple distorted images of the background object. This phenomenon is known as strong gravitational lensing and over the past years has proven to be a powerful tool for measuring the mass distribution of galaxies, groups and clusters of galaxies.

The presence of a low-mass substructure within the main lensing galaxy or of a small halo along the line-of-sight will affect the gravitational potential locally, which in turn, will locally affect the properties of the lensed images from what is expected to be produced by a globally smooth mass distribution. The strength of this effect is dependent on the mass of the (sub)structure and its position relative to the lensed images.



Cold Dark Matter

CDM - Stars

Warm Dark Matter

*Figure 1 - The predicted amount of substructures for different dark matter models (Lovell et al. 2012). Left, the dark matter distribution in a Milky-Way type of halo in a CDM simulation. Centre, the distribution of stars in a Milky-Way type of halo in a CDM+baryons simulation. Right, the dark matter distribution in a Milky-Way type of halo in a WDM simulation. There are significant differences in the abundance of the substructure between the CDM and WDM models. Also, tracing the substructure through their stellar emission is insufficient to detect the lowest mass haloes, where the CDM and WDM models most strongly diverge.*

A clear example of this phenomena, although at higher masses than one would like to target, is the lens system known as “the Clone” (Figure 3). In the Clone, the long lensed arc is clearly perturbed – it splits and bends – at the location of the “substructure” in this system, which is galaxy G4. Crucially, both the location and the mass of G4 are given by the behaviour of the lensed emission, and this detection and mass measurement would have been made even if G4 were purely dark. Of course, in this case, both the main halo and the substructure (G4) are relatively massive, with G4 having a mass of about  $3 \times 10^{10}$  solar masses (Vegetti et al. 2010a), making the perturbation of the arc clearly visible to the eye. For sub-galactic scale structures, both high resolution and sophisticated modelling are needed for the detection. For example, Vegetti & Koopmans 2009a have developed a unique Bayesian gravitational lens modelling technique called *gravitational imaging* that allows one to detect dark (sub)structures in distant galaxies and along their line-of-sight via their gravitational effect on highly magnified Einstein rings.

**Current constraints on the dark matter mass function:** To date there have been only 3 published detections based on this technique. Vegetti et al. 2010b have reported the first detection of a low-mass dark substructure at redshift of 0.2 from HST-ACS imaging and then later, Vegetti et al. 2012 have reported the detection of a dark substructure in a lens galaxy at redshift 0.881 from Keck-AO imaging (and confirmed by independent Keck filters and HST data). With a mass as low as the Sagittarius satellite in the Milky Way, this is the smallest and farthest substructure currently known. More recently, Hezaveh et al. 2016, using high resolution data from the ALMA long baseline campaign, have reported the detection of a  $10^9$  solar masses substructure at redshift 0.3. At the same time, non-detections still provide a statistically interesting constraint on the dark-matter mass function. Using both detections and non-detections for a sample of 11 lenses observed with the HST, Vegetti et al. 2014 have obtained the first observational constraint on the substructure mass function beyond the Local Group ( $z \sim 0.2$ ) and derived a mass fraction in substructure of  $f = 0.0064 \pm 0.0080$  at the 68% confidence level. These results are consistent with predictions from the dark-matter-only and hydro EAGLE simulations (Despali & Vegetti 2017). Due to the relative high masses probed, current observational limits are in agreement with prediction from CDM but do not rule out WDM models. To this end it is necessary to decrease the detection threshold (i.e. reduce the smallest detectable mass) to  $10^8$  arcsec

solar masses and below, where CDM and WDM predictions differ significantly (Figure 2).

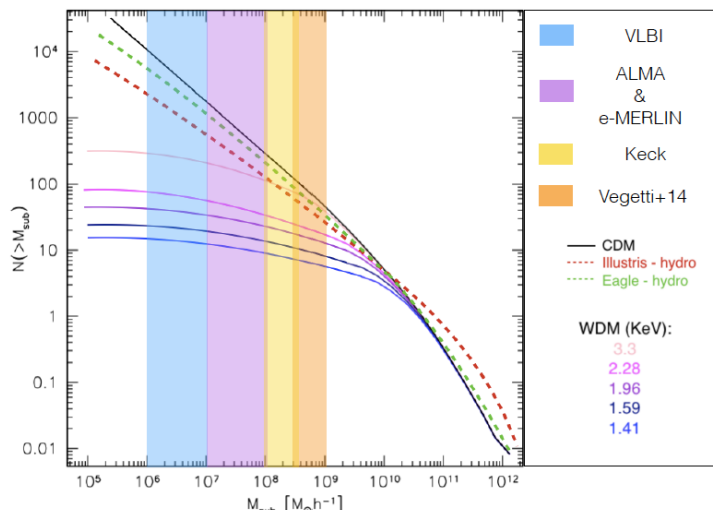


*Figure 2 - The predicted substructure mass function from CDM only simulations (black solid line), from the hydrodynamical simulations EAGLE (dashed green line) and Illustris (dashed red line) and from different WDM models (pink, purple, dark blue and light blue lines) with (dashed lines) and without (solid lines) baryons. The shaded areas show the mass regime that can be probed by different telescopes.*

**Contribution from the line-of-sight:** Up to now, most comparisons between theoretical predictions and observations have focused on the substructure (i.e. small-mass haloes gravitationally bound to the host lens galaxy) mass function. However, CDM and WDM models make clear predictions for the halo mass function in general. At the same time, gravitational lensing is sensitive to the presence of small-mass haloes both in the lensing galaxies and along their entire line-of-sight (LOS). As demonstrated by Despali, Vegetti & White (2017), the contribution from small-mass haloes along the LOS is important for two reasons: (1) as the lensing effect depends on the redshift of the perturber, small LOS haloes that are located at a lower redshift than the main lens produce larger perturbations of the lensed images than substructures of the same mass inside the lens galaxy, meaning that the detection threshold is effectively lower for foreground objects (Figure 4); (2) depending on the redshift of the lens and the smallest detectable mass, the number of detectable LOS haloes can be larger or equal to the number of detectable subhaloes (Despali, Vegetti & White 2017). The LOS represents therefore an important contribution that can significantly boost the number of observable small-mass haloes and, therefore, together with substructures provide tighter constraints on the dark-matter mass function.

**Detection threshold:** In the *gravitational imaging* approach, the lowest detectable mass is set by (1) the angular resolution of the imaging, (2) the signal-to-noise ratio of the lensed arc, and (3) the clumpiness of the surface brightness distribution in the lensed source. Below, we discuss in more details the role played by points (1) and (3) for a given signal-to-noise ratio.

**On the angular resolution:** Mass substructures within the lensing galaxy and LOS haloes produce a local distortion of the lensed images at a scale that is comparable or slightly larger than their Einstein radius. For these objects to be detected observations with angular resolutions smaller or comparable to their Einstein radius are therefore required. Figure 2, highlights the mass regime that can be currently probed by different telescopes based on

their angular resolution. As demonstrated by Lagattuta et al. 2012 and Vegetti et al. 2012, observations with the Keck AO system (resolution of 65 mas) can improve the sensitivity to mass substructure relatively to HST (resolution 100 mas) by almost an order of magnitude and reach a substructure mass limit around  $10^8$  solar masses. A further improvement in sensitivity can be then obtained with interferometric observations with ALMA (35 mas) and e-MERLIN (50-150 mas). To probe the dark matter mass function at the very low-mass end around  $10^6$  solar masses observations at an angular resolution of only a few milli-arcseconds or better are needed. This is because a substructure with a mass of  $10^6$  solar masses will produce an Einstein ring with a radius of just 3 milli-arcseconds, or at least distortions on this angular-scale. At present, such high angular resolutions (1-50 mas) can only be achieved using Very Long Baseline Interferometry (VLBI) observations of extended gravitational arcs at cm- and mm-wavelengths (Figure 5; Spingola et al. 2017). However, interferometric observations are limited by the number of lensed sources with extended structure at these scales. Hence, high substructure sensitivity can only be reached for a handful of objects (McKean et al. 2017). In the future, observations with the European Extremely Large Telescope (E-ELT) using the MICADO adaptive optics system will approach this desired resolution at 1.1  $\mu$ m.

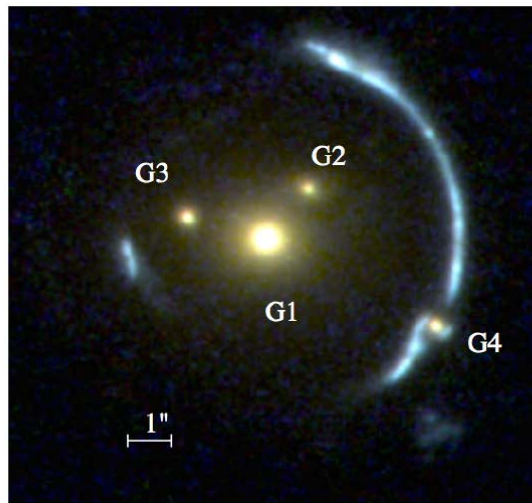


*Figure 3 - Overview of the lens system SDSS J120602.09+514229.5 (the Clone). The luminous satellite G4 is locally distorting the observed lensed emission in correspondence of its location in a way that depends on its mass and that would be observable even if G4 were completely dark. Surface brightness perturbations of lensed arcs by small substructure provide a gravitational probe on the dark matter mass function.*

*On the complexity of the source:* This point arises because the presence of the (sub)structure changes slightly the location of the lensed emission in the arc. These small shifts in location are easier to see if the surface brightness of the lensed object has strong gradients in it, rather than being a smooth distribution. More precisely, as showed by Koopmans (2005), the strength of a surface brightness anomaly ( $\delta I$ ) due to a potential perturbation is  $\delta I = -\nabla S \cdot \nabla \delta \psi$ , i.e. the inner product of the gradient of the source brightness distribution ( $\nabla S$ ; evaluated in the source plane) dotted with the gradient of the potential perturbation due to (sub)structure ( $\nabla \delta \psi$ ; evaluated in the image plane). The anomaly detection threshold for a given signal-to-noise ratio and angular resolution thus effectively depends on two conditions: the mass of the (sub)structure (be it luminous or dark) and the level of surface brightness structure of the source (to first order its rms). An

increase in either results in an increase in the observed surface brightness anomaly. Hence, mass (sub)structure can be detected more easily for sources that are highly structured (i.e. large values of  $|\nabla S|$ ) or, conversely, more structured sources afford a lower mass detection threshold for a fixed signal-to-noise ratio (see Figure 6). Whereas Nature provides us with a lens and possibly (sub)structure, the observer can choose the optimal filter through which the system is observed. By observing lensed arcs and Einstein rings in bluer bands, their surface brightness variations (due to star-formation) are substantially enhanced compared to observing older and smoother stellar populations in the IR. This either substantially increases the substructure detection significance or, conversely, significantly lowers the mass-threshold for detecting low-mass (sub)structures. For example, HST imaging with WFC3-F390W can reach (sub)structure masses as low as what is possible with Keck AO despite the lower angular resolution.

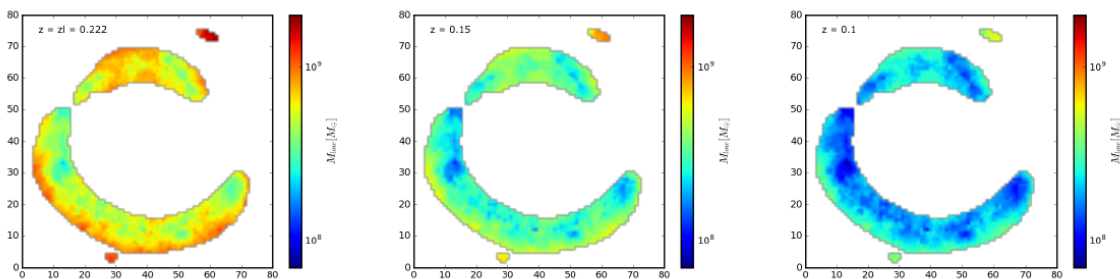


*Figure 4 - Lowest detectable mass as a function of position for substructures (left panel) and for LOS haloes with the same projected position and located at different redshifts (middle and right panels).*

### 3.6.2 Pushing down the mass function with a new optical instrument

An 8-metre diffraction limited telescope in V-band would be a key instrument for the detection of small-mass dark matter haloes for several reasons. First, the resolution (comparable to what will be achieved with the E-ELT), combined with the extra boost in (sub)structure sensitivity provided by the complex morphology of the data in this band would represent a significant improvement over both the HST and Keck AO, but potentially the E-ELT as well. In particular, given the expected angular resolution and taking into account the possibility to target clumpy lensed sources, it is expected that such an instrument would allow one to detect substructure masses around  $10^7$  solar masses and therefore foreground dark matter haloes of about  $10^6$  solar masses.

As gravitational lens systems with blue star forming sources are easier to find with both morphological and spectroscopical techniques, observations with an optical camera would not be limited by small sample sizes, unlike current interferometric observations at cm- and mm-wavelengths. For example, it is expected that Euclid will lead to the discovery of hundred-thousands of new gravitationally lensed objects.

In Figure 7, we show the constraints on the dark-matter mass function parameters that one is expected to derive from different samples of gravitational lens systems with sensitivity to (sub)structure masses around  $10^7$  solar masses. With such a high sensitivity, all relevant parameters could be tightly constrained with a relative small sample of 30 gravitational lens systems.

Moreover, the possibility of several filters would allow one to target star forming lensed

galaxies between redshift 2 to 5. Provided that a good enough sensitivity and resolution can be maintained at all bands, this not only would allow one to maximise the volume of the probed line-of-sight and therefore the number of small-mass detectable objects, but it would also allow one to study how the dark-matter mass function evolves across cosmic time.

Finally, a synergy with the E-ELT could allow to confirm potential detections across filters and reliably exclude potential false positives.

### 3.6.3 Technical Requirements

Here we discuss the key technical requirements for probing the dark-matter mass function with gravitational lens systems. The main key ingredient is the angular resolution which in order to provide a clear improvement over the HST and Keck AO and to be competitive with current mm and sub-mm interferometers has to be comparable with what will be achieved with the E-ELT/MICADO. This has to be matched by high sensitivity to compensate for the loss of signal-to-noise ratio due to the increased resolution, ideally one would like to maintain a signal-to-noise ratio of at least 10 across the extended emission of the lensed images without excessive use of telescope resources.

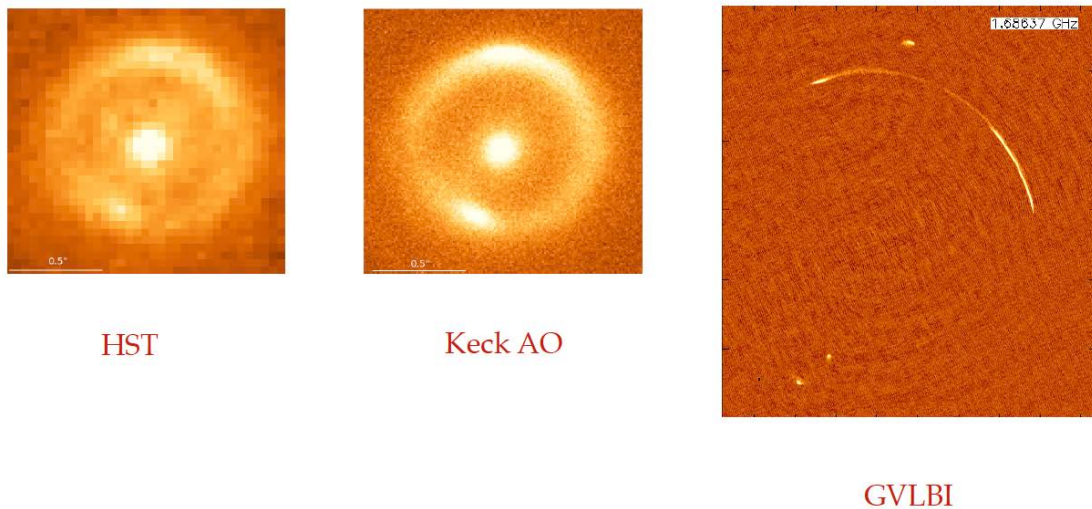


*Figure 5 - Increased sensitivity to substructure from high resolution imaging. Data for the gravitational lens system B1938+666 from the HST (left), Keck adaptive optics (centre) and cm-wavelength global Very Long Baseline Interferometry (right). The angular resolution of the imaging data increases from 150 mas (left), to 65 mas (centre), to 2 mas (right); correspondingly the detection threshold for substructure detection decreases from  $10^8$  to  $10^6 M_{\text{sun}}$ .*

As the main targets would be galaxy-galaxy strong gravitational lenses, the angular separation of the lensed images are expected to be between 1 and 5 arcseconds, hence a large field-of-view is not a strict requirement, provided that is large enough to image all multiple lensed images at the same time. Fail to do so would render the gravitational technique inapplicable as the redundancy provided by the multiple images is the basic requirement for the detection of small-mass haloes via their gravitational effect.

As the sensitivity to small-mass haloes can be significantly boosted by targeting star forming galaxies, observations in bands V to Z would be important to detect the smallest halo masses, probe the evolution of the dark-matter mass function and minimise the required

sample size by maximising the line-of-sight volume.

As one could target known gravitational lens systems with measured redshift, spectroscopy is not a strong requirement.

### 3.6.4 Summary

Measuring the dark-matter mass function represents a key observational probe of the nature of dark matter. While most of small-mass galaxies are too faint or even dark to be directly observed, gravitational lensing provides a powerful method to detect small-mass haloes in gravitational lens galaxies and along their line-of-sight. A new optical VLT V-band diffraction limited optical camera would provide a significant step forward relatively to current constraints obtainable with the HST and Keck AO and would allow one to clearly confirm or rule out CDM.

**References:** Despali G. & Vegetti S., 2017 arXiv-1608.06938; Despali G. Vegetti S. & White D.M in prep.; Hezaveh Y.D., et al., 2016, ApJ, 823, 37; McKean et al. 2017 in prep.; Koopmans L.V.E., 2005, MNRAS, 363, 1136; Lovell et al., 2012, MNRAS, 420, 2318; Planck Collaboration, 2016, A&A, 594, A1; Springola et al. 2017 in prep.; Vegetti S. & Koopmans L.V.E., 2009a; Vegetti S., et al., 2010, MNRAS, 408, 1969; Vegetti S., et al., 2010, MNRAS, 407, 225; Vegetti S., et al., 2012, Nature, 481, 341; Vegetti S., et al., 2014, MNRAS, 442, 2017.

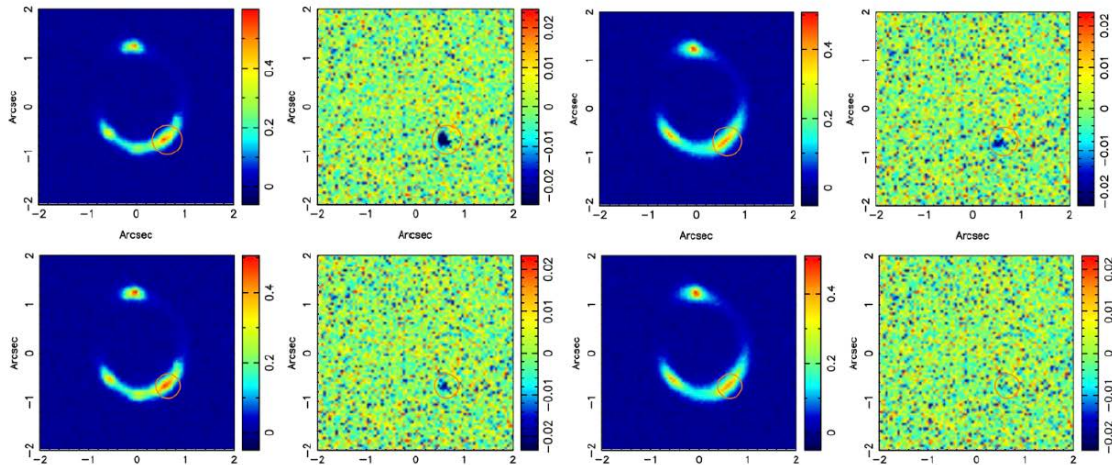
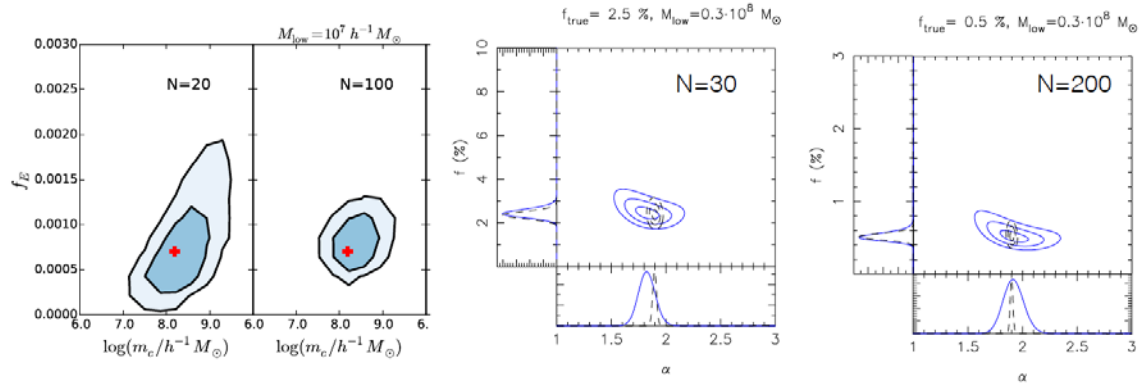


Figure 6 - Left (2x2) panels: Clumpy source with 5 star-clusters. Top: A substructure of  $10^8$  (top) or  $3 \times 10^7$  (bottom) solar mass is placed on the ring causing an anomaly (right) in the surface brightness. Right (2x2) panels: Idem for a smooth source. Note that for a similar mass the anomaly is much larger for the more clumpy source.



*Figure 7 - Expected constraints on the mass function parameters: dark matter fraction in (sub)structures  $f$ , mass function slope  $\alpha$  and cut-off mass  $m_c$  from different sample sizes with sensitivity between  $10^7$  and  $3 \times 10^7$  solar masses.*



## 3.7 Star formation science with an optical AO instrument at the VLT

By Monika Petr-Gotzens, ESO, Garching bei München, Germany

### 3.7.1 The formation of multiple stars

Binary and multiple stars are a frequent result of the star formation process. Two main formation channels are proposed, fragmentation during the pre-stellar core collapse and/or formation via disk fragmentation due to gravitational instabilities. The latter was initially less favoured, since circumstellar protoplanetary disks were thought to be too hot and not massive enough to permit disk fragmentation. But there is accumulating new evidence from observations (Tobin et al. 2016) as well as from theory (Lomax et al. 2015) that disk fragmentation could actually be the main responsible for the formation of binaries and multiples on small scales. Here, small scales refer to separations of less than  $\sim$ 100AU (Figure 1). This is, in fact, the range in separation where most young pre-main sequence stars host a companion (Duchene & Kraus 2013), as proven by numerous observational studies employing high spatial resolution imaging (HST or near-infrared AO) on nearby star forming regions (e.g. Lafreniere, 2014; Köhler et al. 2006; Padgett et al. 1997). Those studies, however, are restricted to probing physical binary separations of 10 - 40 AU, while the full details of the shape of the separation distribution down to a 1 AU or less is crucially important to understand the star formation process. Only dynamically pristine young pre-main sequence binaries hold clues to the formation process. In dense stellar clusters, such as the Orion Nebula Cluster, it would be only tighter, i.e.  $<50$ AU, binaries that can survive early dynamical disruptions through stellar encounters. Diffraction-limited optical AO imaging providing spatial resolutions of  $\sim$ 0.02" - 0.03" will enable us to probe such close binaries for the first time. For the closest star forming regions at a distance of  $\sim$ 130 AU one would be sensitive to companions as close as 2-3 AU, and thereby closing the remaining gap to spectroscopic binaries (Figure 2).

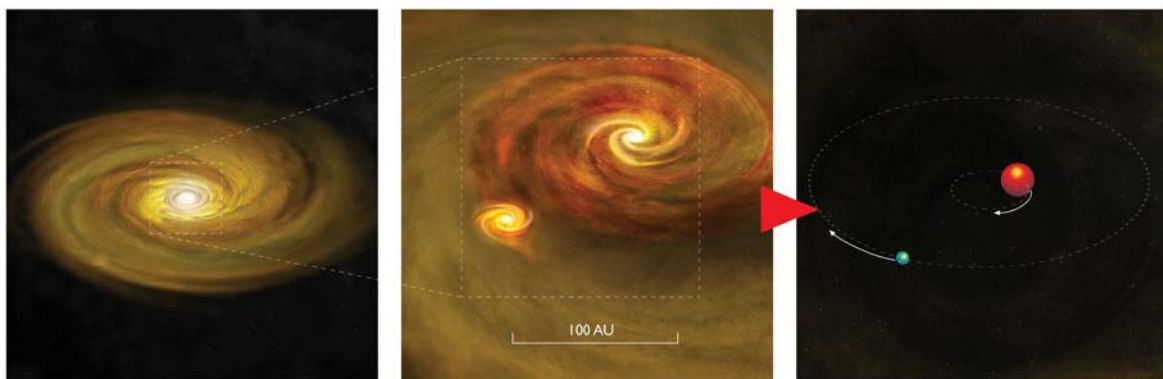


*Figure 1: Sketch of binary star formation from gravitational disk instability. This process governs the formation of multiples at separations of <100AU. The final binary system could settle at even smaller separation due to dynamical evolution during the pre-main sequence phase.*

For a FOV of the optical AO imager as large as  $30'' - 40''$ , there are typically 4-7 pre-main sequence stars in a single FOV, considering typical young Galactic stellar cluster densities as in Orion or the Ophiuchus cluster, which would enormously increase the observing efficiency compared to "one star at a time" observing. Also, pre-main sequence stars are intrinsically red which means that wavefront sensing in the near-infrared is an absolute advantage for this kind of science, while the optical brightness of pre-main sequence stars would still be within reach for an 8m telescope as the increase in spatial resolution similarly improves the sensitivity.

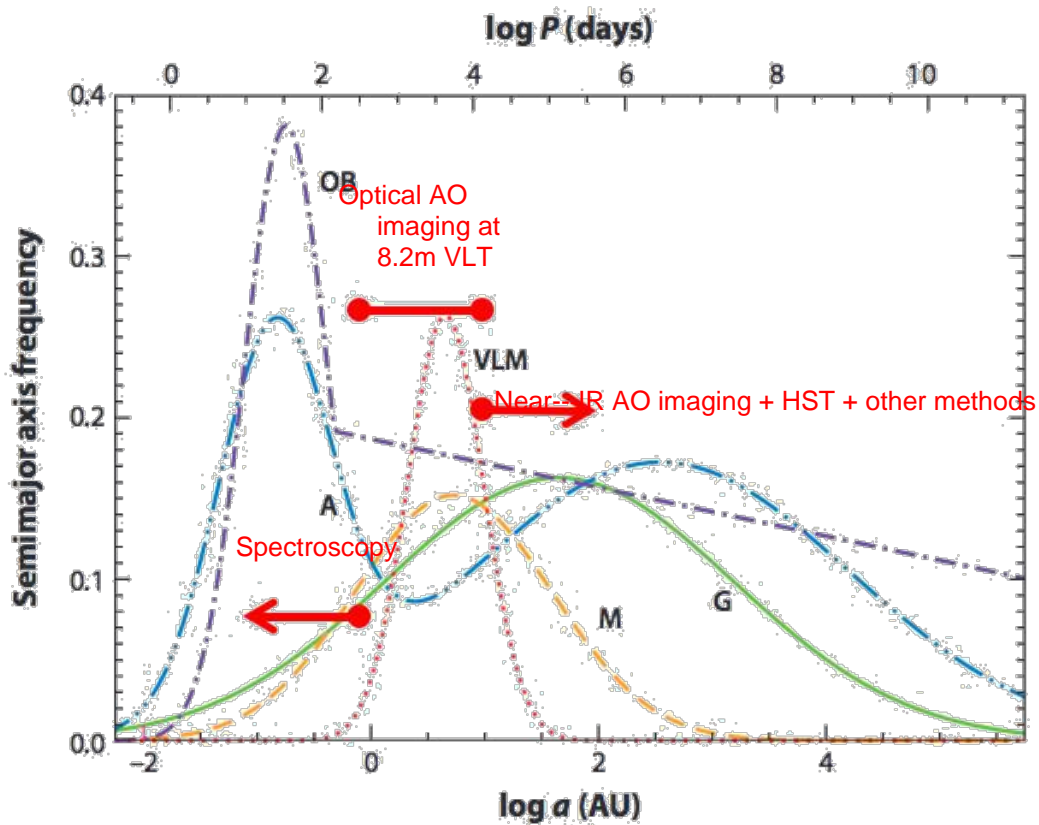


*Figure 2: The observed binary separation distribution for different types of main sequence stars. Optical AO imaging could fill in the very poorly studied regime of close binaries with separations 1-10 AU (for nearest star forming regions) or 5-50 AU (for Orion, the closest high mass star forming region). Figure adapted from Duchene & Kraus 2013.*

Typical H-band magnitudes of potential target stars in young clusters and associations with ages  $<4$  Myr are  $H < 14$  mag for sources located at distances up to Orion (400 pc). Extinction plays a minor role as long as sources are not extremely embedded (e.g.  $A_V > 10^m$ ). For any less extinguished source V-band magnitudes are expected in the range  $19 < V < 27$ . In order to be sensitive to very low mass companions close to solar-like stars the sensitivity of a new instrument should ideally be  $\Delta m < 4$  mag as close as  $0.02''$ .

Since ALMA is starting to explore the circumstellar environment at similar spatial scales (few AUs) the proposed observations would be a perfect complement towards the overall goal to understand multiple star formation.

Regarding the choice of filters, it is important to have broad-band filters from V to I in order to estimate the stellar types. But also, an Halpha narrow-band filter would be very useful, since young pre-main sequence stars are often still accreting from their circumstellar disk, which manifests in typically strong H $\alpha$  emission. At spatial resolutions of 1AU new studies of accretion strength from individual binary components and their associated emission line jets could be made.

### 3.7.2 Star formation in the LMC

The Large and Small Magellanic Cloud are our nearest galaxy neighbours that are actively forming stars, hence they offer a unique opportunity to study the star formation process in an environment different from our own Galaxy. As the LMC and SMC are significantly more metal-poor than the Milky Way, that is 2.5 and 5 times respectively lower than Solar (Westerlund 1997, Venn 1999), they do also provide a superb local template for star formation studies of the early universe. At a distance of the LMC of  $\sim$ 50kpc it is however indispensable to employ the highest possible spatial resolution in order to resolve young stellar clusters and star forming aggregates into individual stars. Hubble Space Telescope (HST) observations are currently the most suitable tool in terms of spatial resolution and sensitivity for studying low mass pre-main sequence stars in the LMC. Da Rio et al. (2009) utilized deep HST optical photometry to investigate the initial stellar mass function of LH 95, a young populous LMC association (Figure 3). This analysis describes the by far deepest, and highest spatial resolution, observation of any young stellar cluster in the LMC, and traces the initial stellar mass function reliably down to  $\sim$ 0.4M<sub>SUN</sub>. Yet, HST's resolution is a few thousand AU only, i.e. individual cluster stars are barely resolved, presuming that the cluster displays a similar stellar density as Galactic clusters, i.e.  $10^3$  -  $10^4$  stars/pc<sup>3</sup>. Down to  $\sim$ 0.4M<sub>SUN</sub> da Rio et al. (2009) find no significant differences for the IMF of LH 95 compared to Galactic clusters' IMFs, supporting an universal star formation law. This might be not surprising, because even in our Milky Way the most noticeable IMF differences show up at masses lower than the peak of the IMF which is typically around 0.2 - 0.4M<sub>SUN</sub> (e.g. Bastian et al. 2010).

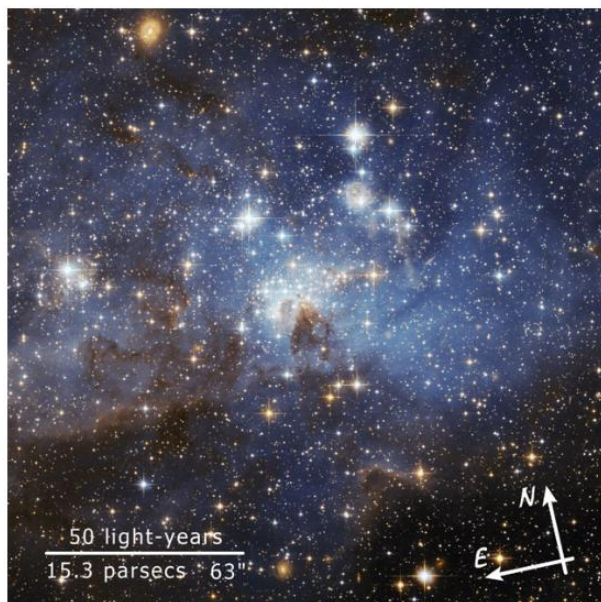


*Figure 3: HST optical image of the young stellar cluster LH95 in the LMC. It is a composite of V-filter and I-filter observations obtained with the HST Advanced Camera for Surveys.*



With optical AO at the 8.2m VLT it would be possible to achieve unprecedented spatial resolution *and* sensitivity over a reasonably large FOV. Assuming optical AO delivers 20mas resolution imaging this is a factor of 3(!) better than the HST and for the first time one can truly resolve individual stellar sources in LMC stellar clusters. Targeting sensitivities of V and I of approximately 30mag would be an important step towards sampling the peak of the IMF where differences between metal-poor LMC clusters and the Galaxy start to emerge. Note that a FOV of ~40" would sufficiently encompass the centers of LMC clusters including several hundreds of pre-main sequence stars (see also Figure 3). On the technical side, there are usually a handful bright stars with JHK magnitudes brighter than 15mag present within 1arcmin of the centers of young stellar clusters in the LMC that could be used for wavefront sensing.

#### References:

- Bastian, N., Covey, K. R., Meyer, M. R., 2010, ARA&A 48, 339  
Da Rio, N., Gouliermis, D. A., Henning, T. et al. 2009, ApJ 696, 528  
Duchene, G. & Kraus, A., 2013 ARA&A 51, 269  
Köhler, R., Petr-Gotzens, M. G., McCaughrean, M. J. et al. 2006, A&A 458, 461  
Lafreniere, D., Jayawardhana, R., van Kerwijk, M. H. et al. 2014, ApJ 785, 47 Lomax, O., Whitworth, A. P., Hubber, D. A. et al. 2015, MNRAS 447, 1550 Padgett, D. L., Strom, S.E. & Ghez, A. 1997, ApJ 477, 705  
Tobin, J. J., Kratter, K. M., Persson, M. V., et al. 2016, Nature 538, 483  
Venn, K. A. 1999, ApJ 518, 405  
Westerlund, B. E. 1997, macl.book "The Magellanic Clouds"



## 4. Summary of science requirements

This section summarizes the requirements derived from the science cases. In addition to the written cases in Section 3 several discussions were carried out and are reflected in this section. The overall leading science case is presented in Section 3.1 while a collection of other science is presented in the following. It is clear that the instrument is more of the type of a “workhorse” and this document does not present all the possible science cases. For example, time-resolution like science cases are currently omitted.

### 4.1 Place of installation

The VAOI shall be installed at UT4 because it is the only VLT telescope with the AOF infrastructure to host an instrument with advanced visible AO facilities. The available location is the Nasmyth A platform to replace Hawk-I.

### 4.2 Observing modes

The science cases demonstrate that VAOI shall perform imaging shortwards of 1 micron (diffraction limited at V-band with Strehl ratios of >15%) to the blue atmospheric cut off (~320nm) and perform (IFU-) spectroscopy in a similar wavelength range (see Sections 3.3, 3.5). Emphasis is given to V-, R- and I-bands while bluer (to the atmospheric cut off) and redder (up to 1 micron) wavelengths will be dealt with at a best effort basis. At about 800nm and redder ELT instruments will perform better both in spatial resolution and light collecting power.

### 4.3 Adaptive optics

VAOI shall make use of the AOF at VLT/UT4 with potential additional resources as determined in Phase A (e.g. additional DMs) to enable diffraction limited imaging and spectroscopy with Strehl ratios of >15% in V-band over the full science FoV (see e.g. 3.1 and other science cases). A high temporal stability (see also Section 4.9) of the PSF and a significant Strehl ratio in V-band is needed for efficient PSF calibration and high contrast for all science cases.

Proper motion studies require stabilities (i.e. known distortions not changing) over several years or otherwise means of detecting sub-pixel movements over years (see 3.1 and 3.4).

Also, for all science cases the need for a combination of natural AO guide stars (up to three stars covering an area of up to 2 arcmin diameter - TBC) and at least 4 laser guide stars are needed to achieve the science requirements over the full science FoV.

Sky coverage is an important requirement and it shall be >50% in galactic pole regions (see 3.1 and other science cases). To be studied further during Phase A.

The possibility to reconstruct PSFs is strongly desired and delivers the promise to improve the interpretation of science data and thus shall be part of the development plan right from the start (see 3.1 and other science cases).



## 4.4 Scientific filters and spectral resolution

The VAOI imager shall host a minimum of 7 slots for the broad-band filters (U, B, V, R, I, and z or Sloan equivalent) and >10 (TBC) slots for narrow band filters. The focus here is on V- to I-band to allow diffraction limited images from the ground, but also bluer filters are scientifically interesting at a reduced AO performance (still better than seeing limited; however, maybe with a reduced FoV). The full coverage of the wavelength regime up to 1 micron seems beneficial with the same instrument.

The final filter list of the VAOI instrument will be defined at a later stage.

The VAOI spectrograph shall cover wavelengths from the blue ([OII] emission lines at 3727 Å) to about 850 nm (~1 octave) at a spectral resolution of above R ~5000 (the science case in 3.1 would argue for even higher spectral resolution of R>10000 perhaps at reduced wavelength coverage). Ideal for spectroscopy would be an IFU to allow covering a reasonable FoV for single objects (see also Section 4.5).

Imaging and spectroscopy ETCs will have to be designed during Phase A.

## 4.5 Pixel scales and FoV sizes

The VAOI imager shall provide diffraction-limited images in V-band resulting in a resolution element of 17 mas to be sampled with a minimum of 2.3 pixels so 7-8 mas per pixel. The science case demands a minimum field size of about 30 arcsec diameter for the imager (see all science cases).

The spectrograph shall cover a region around a single source with a small IFU. It shall make use of the diffraction limited capabilities of the instrument so a central location in the FOV seems feasible (see 3.1, 3.3, 3.5). For the IFU the minimum FoV is 3" diameter at spaxel sizes of roughly 20 - 40 mas (150x150 – 75x75 spaxels; R-band – diffraction limit = 20 mas). Since the small IFU can be fully used by some targets it would be beneficial (e.g., see Section 3.3) if this instrument allows to obtain simultaneously information on the sky by having a separate sky “aperture”.

## 4.6 Wave-front sensors

In order to maximise the number of science photons the wave front detector (for TT stars) wavelength shall be in the near IR. For the science case of Star Formation (see section 3.7) it is absolutely essential to go IR since all stars in the optical regime are too faint. For all the other science cases an IR WFS does not present any disadvantage, the stars PSF are rather expected to be “sharper” in the near IR.

## 4.7 Optical distortions

Several science cases demand good (to very good) optical performance on the 1/10 of a pixel size accuracy i.e. ~1 mas (see 3.1, 3.4) or better.



## 4.8 Detector

The maximum pixel size of 7 mas results into a size of at least ~4300 pixels for 30 arcsec diameter FoV i.e. a  $\geq 5\text{Kx}5\text{K}$  detector which are readily available on the market. They can be bought to be quantum efficient from about 350 – 900 nm.

The science detector of VAOI shall be operated so that quantum efficiency, read-out-noise, and cosmetics are all optimized.

The focus is on V-, R- and I-band imaging (peak in detector sensitivity; 3.1), however, the detector shall be also sensitive to bluer wavelength.

The spectrograph in an IFU version may lead to high detector area demands. This will have to be analysed during the Phase A design which may lead to a demand of more than one detector.

## 4.9 Integration times and depth

For imaging, integration times are driven by achieving good S/N in a few exposures on faint (e.g.,  $V=$ ~28-30) sources and keeping a stable AO performance over the exposure(s) (see 3.1). Exposure times for single images are estimated to be a few min to 15 min.

Additionally, the detector shall perform well for spectroscopy with somewhat extended total exposure times (roughly factor of 10 or more for total exposure times compared to imaging). The option of separate detector(s) for spectroscopy should be evaluated as part of Phase A.

--- End of document ---